Development of a Novel Sample Preparation Method for Bioarchaeological Proteomics

by

Dylan Multari

Bachelor of Archaeology

Principal Supervisor: Professor Paul A. Haynes,

Department of Molecular Sciences

Associate Supervisor: Associate Professor Ronika K. Power,

Department of Ancient History

This thesis is submitted in partial fulfilment of the graduating criteria for the Masters of Research

Department of Molecular Sciences

Faculty of Science and Engineering

Macquarie University, Sydney, New South Wales, Australia

25 October, 2019

“The life of the dead is placed in the memory of the living.”

- *Marcus Tullius Cicero*

Aut inveniam viam aut faciam.
“I will either find a way, or make one.”

- *Hannibal Barca*

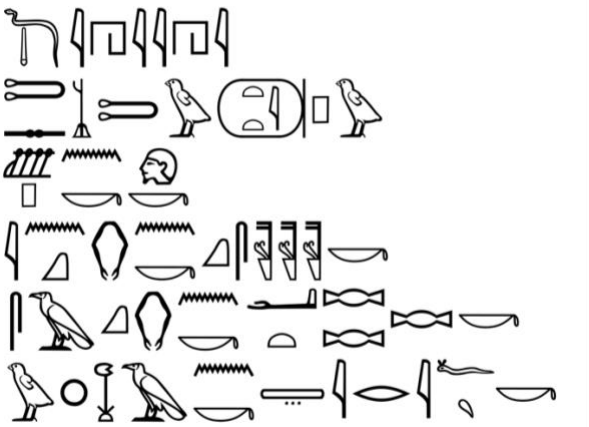

“Rise up, O Teti!
Take your head, collect your bones,
Gather your limbs, shake the earth from your flesh!”

- *Pyramid Texts of Teti I, Saqqara, Utterance 373*

Declaration

I certify that this thesis entitled ‘Development of a Novel Sample Preparation Method for Bioarchaeological Proteomics’ is an original piece of my research work. No part of this thesis has been submitted to any other institution towards a component of a degree or award. Any form of assistance received towards this research work has been duly acknowledged. I certify that all information sources and literature have been referenced in this thesis.

Dylan Multari
25 October, 2019

Contents

Acknowledgements ..... *vi*

Abstract ..... *vii*

Ethics Statement ..... *viii*

List of Terms and Abbreviations ..... *ix*

1 Introduction *1*

1.1 Bioarchaeology **1**

1.2 Importance of scientific studies of archaeological materials **1**

1.3 Ancient DNA analysis **2**

1.3.1 Advantages of aDNA 2

1.3.2 Problems with aDNA-based approaches 4

1.4 Ancient proteomics **5**

1.4.1 Advantages of proteins over DNA 5

1.4.2 Proteomic analysis of 500-year-old Incan Mummies 5

1.4.3 Proteomic analysis of 4200-year-old Egyptian Mummies 6

1.4.4 Proteomic analysis of 2000-year-old Osteogenic Sarcoma 6

1.4.5 Analysis of ancient bone collagen fingerprinting as radiocarbon screening and species identification tool 7

1.4.6 Proteomic analysis of an Iñupiat potsherd 8

1.4.7 Protein Deamidation as potential dating tool 9

1.4.8 Sex estimation using amelogenin protein fragments 10

1.5 Paleoproteomics and phylogeny **10**

1.5.1 Soft-tissue preservation in fossilised remains 11

1.5.2 Proteomic analysis of *Tyrannosaurus Rex* femur 11

1.5.3 Analysis of unidentified Cretaceous Period therapod dinosaurs 12

1.5.4 Proteomic analysis of Mammoth and Mastodon collagen sequences in bones and fossils 13

1.6 Non-invasive analysis of archaeological materials **13**

1.6.1 Non-invasive sampling and bioarchaeology 15

1.7 Skin sampling strips **15**

1.8 Aims and scope of this thesis **16**

2 Methodology *17*

2.1 Application of skin sampling strips to modern samples **17**

2.2 Mer-Neith-it-es Remains **17**

2.3 Application of skin sampling strips to ancient samples **18**

2.4 Extraction of proteins from skin sampling strips **23**

2.5 SDS-PAGE of strip extracts **23**

2.6 Trypsin in-gel digestion **23**

2.7 NanoLC-MS/MS of peptide extracts **24**

2.8 Protein Identification using X! Tandem **24**

2.9 Calculating False Discovery Rate at Protein and Peptide level **24**

2.10 Functional categorisation of identified proteins **25**

3 Results and Discussion 26

3.1 Development of protein extraction protocol from skin sampling strips 26

3.1.1 Proteomic analysis of modern strip samples 27

3.2 Protein identification of ancient bone samples 29

3.2.1 Proteomic analysis of humeral shaft 29

3.2.2 Proteomic analysis of exposed tibia 30

3.2.3 Proteomic analysis of mandible interior 31

3.2.4 Proteomic analysis of mandible exterior 32

3.2.5 Proteomic analysis of molar 32

3.3 Proteomic analysis of ancient skull fragment samples 32

3.3.1 Skull fragment 1034 interior 33

3.3.2 Skull fragment 1034 exterior 33

3.3.3 Skull fragment 1134 interior 34

3.3.4 Skull fragment 1134 exterior 35

3.3.5 Skull fragment 1443 interior 36

3.3.6 Skull fragment 1443 exterior 36

3.3.7 Skull fragment 1459 interior 37

3.3.8 Skull fragment 1459 exterior 38

3.3.9 Skull fragment 1439 interior 38

3.3.10 Skull fragment 1439 exterior 39

3.3.11 Skull fragment 1476 interior 40

3.3.12 Skull fragment 1476 exterior 41

3.3.13 Skull fragment 549 interior 42

3.3.14 Skull fragment 549 exterior 42

3.3.15 Skull fragment 559 interior 43

3.3.16 Skull fragment 559 exterior 44

3.4 Overall summary of protein identifications from all ancient skull and bone samples 45

4 Conclusion and Future Directions 47

4.1 Successful proof of concept 47

4.2 Ideas for further improving the sampling method 47

4.3 Ideas for further developing the data analysis method 48

4.4 Ancient remains and non-invasive sampling 49

4.5 Finding out more about the enigmatic Mer-Neith-it-es 49

4.6 Conclusions 50

References 51

Appendix 1: CloudStor repository of raw MS/MS files and unfiltered GPM outputs 59

Appendix 2: HREC Ethics Approval Letter 60

Acknowledgements

Firstly, I would like to thank my supervisors for giving me the opportunity to work on this interesting and unique project. My sincere thanks to Paul for his constant support, guidance, and insights, without which this thesis would not be possible. I am grateful for all the time, effort, and resources he has put into supervising and supporting my research. Thanks also to Ronika for her unique perspectives which assisted me in seeing the bigger picture, and of course for her undying enthusiasm and encouragement. Their unwavering confidence in me shone through any doubts and pushed me to work to the best of my abilities always. I am truly grateful to have such inspiring supervisors to guide me in the first steps of my research career.

Thank you to Drs Jamie Fraser and Conni Lord from the Nicholson Museum, University of Sydney for opening up your collection to us and making this unique opportunity a reality. I look forward to any future collaborations with you.

Special thanks to the team at APAF, specifically Drs Ardeshir Amirkhani, Matt Fitzhenry, and Matthew McKay, for their assistance and infinite patience with using and troubleshooting the Q Exactive.

I would like to thank all my labmates, David, Farhad, Fatemah, Liting, Prathiba, and Sara, for all the wisdom, support, and laughs we've shared. It has been an absolute pleasure to work alongside you. I extend my gratitude to my friends and colleagues, Indi, Jane, Julian, Matt, and Michelle, for the countless coffees, drinks, and lunches. You have all made this year a memorable and enjoyable experience. Special thanks also to Paige for tolerating the stress cleaning and lazy dinners.

Finally, I thank my mum, Judie, for always being a phone call away when I needed the extra support and encouragement.

Abstract

Ancient proteomic analysis has been shown to have several advantages over ancient DNA studies, largely due to the ability of proteins to survive over longer periods of time. Typically, sampling of bioarchaeological material for proteomics has involved the use of drills and hammers, which presents an issue when working with museums and other heritage organisations. There are a few studies in the literature on the use of specifically manufactured sampling tapes for the minimally-invasive analysis of paintings and frescoes, but no evidence of their application to human remains.

This thesis deals with the development of a novel minimally-invasive sample preparation technique for application in the mass spectrometric analysis of bioarchaeological materials. By applying commercially available, dermatology-grade skin sampling strips to modern skin surfaces as a surrogate, an extraction protocol was developed, and subsequently applied to numerous skull and bone fragments belonging to a 26th Dynasty Egyptian Mummy in the collection of the Nicholson Museum, University of Sydney, Australia. Extracted proteins were separated on protein gels and in-gel digested, and resulting peptides were analysed by nanoflow liquid chromatography – high resolution tandem mass spectrometry. We have identified keratins and collagens as expected, but have also found a number of ancient intracellular and brain proteins on the skull and bone fragments. This successful proof-of-concept study holds great promise for exciting further optimisation and application.

Ethics Statement

Ethics clearance was not required for the ancient samples analysed in this study as the remains were known to be several thousand years old and no living relatives are known. The Macquarie Unversity Ethics Committee issued a letter of exemption as indicated below. The sampling was conducted by Dylan Multari, Professor Paul A. Haynes, and A/Prof Ronika K. Power, with the express permission of the Nicholson Museum Curator, Dr. Jamie Fraser, and under the supervision of Dr. Conni Lord, Nicholson Museum, University of Sydney, Australia. The remains are part of the permanent Nicholson Museum collection. Figures used in this thesis provided by the Nicholson Museum were used with the express written consent of Dr. Jamie Fraser. The modern samples were collected by Dylan Multari from his own forearm, and are exempt from ethics approval on the grounds of self-experimentation. All research in this thesis was conducted according to the Macquarie Code for the Responsible Conduct of Research, under the supervision of Professor Paul A. Haynes, Department of Molecular Sciences, and A/Prof Ronika K. Power, Department of Ancient History, Macquarie University, Australia.

Ethics approval Reference No: 5201849176758

List of Terms and Abbreviations

ACN – Acetonitrile

aDNA – Ancient DNA

ARCI – Autosomal Recessive Congenital Ichthyosis

ADP – Adenosine diphosphate

ATP – Adenosine triphosphate

BCE – Before Common Era

Ca. – circa

CE – Common Era

CNPD – 2',3'-cyclic-nucleotide 3'-phosphodiesterase

CNS – Central Nervous System

cRAP – Common Repository of Adventitious Proteins

CT – Computed Tomography

DNA – Deoxyribonucleic acid

DTT – Dithiothreitol

ELISA – Enzyme-linked Immunosorbent Assay

ESI – Electrospray Ionisation

FA – Formic acid

FDR – False Discovery Rate

GAPDH – Glyceraldehyde-3-phosphate dehydrogenase

GC – Gas Chromatography

GC-MS – Gas Chromatography Mass Spectrometry

GFAP – Glial Fibrillary Acidic Protein

GO – Gene Ontology

GPM – Global Proteome Machine

GTP – Guanosine triphosphate

HCD – Higher energy Collisional Dissociation

HSP – Heat Shock Protein

IAA – Iodoacetamide

LC – Liquid Chromatography

LC-MS/MS – Liquid Chromatography coupled with tandem Mass Spectrometry

MALDI – Matrix-assisted Laser Desorption/Ionisation

MS – Mass Spectrometry

MS/MS – Tandem Mass Spectrometry

mtDNA – Mitochondrial DNA

nanoLC-MS/MS – Nanoflow Liquid Chromatography coupled with tandem Mass Spectrometry

PBS – Phosphate Buffered Saline

PCR – Polymerase Chain Reaction

PMF – Peptide Mass Fingerprinting

PPIA – Peptidyl-prolyl cis-trans isomerase A

Rpm – revolutions per minute

SDS – Sodium Dodecyl Sulfate

SDS-PAGE – Sodium Dodecyl Sulfate Polyacrylamide Gel Electrophoresis

SEM – Scanning Electron Microscopy

TD/Py-GC-MS – Thermal Desorption/Pyrolysis Gas Chromatography Mass Spectrometry

TOF-SIMS – Time-of-flight Secondary Ion Mass Spectrometry

TRiC – T-complex Protein-1 Ring Complex

VDAC1 – Voltage-dependent Anion-selective Channel Protein 1

ZooMS – Zooarchaeology by Mass Spectrometry

(This page is intentionally left blank)

1 Introduction

1.1 Bioarchaeology

Bioarchaeology is a subdiscipline of archaeological science that concerns itself with the scientific analysis of ancient biological remains through laboratory- and field-based techniques. Historically, these analyses were more physical and were restricted to observational methods such as osteology and histology when dealing with human remains, but the field has begun to incorporate biomolecular methods including genomics and proteomics [1]. Technological developments in a number of scientific fields have led to the advancement of bioarchaeology and the construction of a more conclusive understanding of the past [1, 2]. These studies have been conducted on a wide range of archaeological samples including teeth and dental calculus, buccal swabs, blood, skin, textiles, and ceramics [3-8].

1.2 Importance of scientific studies of archaeological materials

The traditional method of reconstructing the past has been through the gross observation of archaeological materials including artworks, ceramics, and textual evidence. Scientific analysis validates this historical data, whilst also allowing for further information to be obtained. The scientific analysis of archaeological materials has the potential to rewrite history and provide additional, previously unavailable, molecular-scale information about the past, which may be missing from traditional primary sources [1, 9, 10]. Molecular data has been used in the elucidation of past diet, lifestyle, disease, pathology, and phylogeny of ancient human and animal populations, many of which no longer exist [3-7, 11]. Furthermore, bioarchaeological data has informed modern medicine and epidemiology, and has expanded our knowledge of both extant and historic disease states and biomarkers of such conditions [9, 12-14].

Osteology was the first form of bioarchaeological research as the term was initially coined in reference to studies on animal bones from archaeological sites [15]. In most cases, all that remains of a living organism in an archaeological context is the skeleton, which makes it vital for reconstructing the past. Osteological analysis of skeletal remains allows for the determination of species, sex, disease, and sometimes cause of death, especially in the case of interpersonal violence or warfare [2, 16, 17].

Isotopic analysis is a relatively new avenue of osteological research in bioarchaeology that has allowed for more detailed scientific analysis of diet in skeletal remains [17]. A study

into a series of male and female remains excavated from southern Peru elucidated that the staple crop in Incan diet was maize (*Zea mays*), validating historical and archaeobotanical evidence. The analysis was done using the stable carbon isotope $\partial_{13}C$ in bone collagen. It was also found that male bones contained higher $\partial_{13}C$ isotopes than females, which is consistent with models of the Incan societal gender convention of men consuming more maize, in the form of beer, than women [17].

Palaeoparasitology is also an emerging field in bioarchaeology. A 2009 excavation of a medieval abbatial complex (783 – 1159 CE) in Nivelles, Belgium discovered a series of burials with skeletal remains and coprolites [18]. Preliminary analysis of these coprolites revealed signs of geohelminth parasitism in the population. Parasitological analysis confirmed this and revealed the presence of *Ascaris lumbricoides* and *Trichuris trichiura* parasites in the fossilised faecal matter. The high abundance of eggs and parasites in the coprolites indicates that parasitic infection was the cause of death for most of the individuals in the complex [18]. This study highlights the importance and relevance of scientific analyses in archaeology and the detailed novel information that can be discerned from ancient remains.

1.3 Ancient DNA analysis

In recent years, molecular approaches such as genomics, amino acid assays, and proteomics have increasingly been applied to the study of archaeological remains. The use of these methods in the analysis of ancient materials has elucidated archaeologically relevant information that has deepened our understanding of the past in regard to culture, evolution and phylogeny, health, disease, and lifestyle.

1.3.1 Advantages of aDNA

The use of ancient DNA (aDNA) in archaeology has allowed for stringent phylogenetic data to be generated about extinct and extant populations. The first reported study of aDNA was that of the quagga, a zebra-like species (*Equus quagga quagga*) that has reportedly been extinct since the late 19th Century CE [19, 20]. Small DNA sequences were extracted from dried muscle samples from a museum specimen and were amplified using bacterial cloning. Mitochondrial DNA (mtDNA) clones were obtained and sequenced. The quagga sequences were compared to an extant species from the genus *Equus*, the mountain zebra (*Equus zebra*). It was found that both species diverged from a common ancestor approximately 3-4 million years ago [20]. This study was revolutionary in elucidating molecular phylogenetic data from

an extinct species before the prevalence of new technology such as polymerase chain reaction (PCR) approaches.

Neanderthals are the closest known evolutionary relatives to modern-day humans and faced extinction around 30,000 years ago. These hominids appear in the fossil records of Europe, the Middle East, and Western Asia from as early as 400,000 years ago [21]. A collection of non-morphologically significant Neanderthal bones from Vindija Cave in Croatia were drilled for bone powder and screened for Neanderthal mtDNA using PCR to generate a draft genome. When compared to modern human DNA, this draft genome was discovered to be more closely related than previously thought, with modern humans inheriting between 1 to 4% of the Neanderthal genome [21].

A further study into the genetic analysis of Neanderthal dental calculus reconstructed diet, behaviour and disease of the early hominins [11, 22]. This study used shotgun sequencing of aDNA extracted from dental calculus to identify DNA associated with specific plants such as wheats and grains, mushrooms, and moss, and animals such as sheep and woolly rhinoceros that comprised a large part of the diet of the individuals, and the wider population. In addition to this, oral microbiota was identified in the dental calculus, which indicates the introduction and genetic evolution of microorganisms that are found in modern-day humans [11, 22].

The study of past epidemics present in archaeological remains has rewritten the history of such diseases and informed modern approaches to future epidemics [13, 23, 24]. aDNA analysis has been applied to the study of past epidemics in order to identify the etiological agent. Samples of aDNA were extracted from the skeletal remains of Justinian Plague victims (525-680 CE) excavated from a cemetery in Germany. These samples were amplified using PCR and were compared to modern strains of *Yersinia pestis*, a known pathogen responsible for other global epidemics [24]. It was found that *Y. pestis* DNA was present in the skeletal remains and confirmed the role this bacterium has played in the history of human health.

Molecular anthropological approaches to understanding human migrations and origins of Indigenous cultures have been extensively applied to the study of populations across Oceania [25, 26]. Ancient bones dating between the 14th and 17th Century CE were collected from excavations in Temoe Atoll in Eastern Polynesia, and mtDNA was extracted from bone powder for PCR. The amplicons were compared with mtDNA from modern individuals in the region to establish the effects of European colonisation on gene flow and conservation of Melanesian genetic lineage [25]. The study discovered that unique Melanesian Q1 mtDNA sequences identified in ancient samples were maintained in modern descendants, indicating

both the presence of indigenous populations well before European colonisation of the region and the preservation of these sequences in the regional gene pool.

1.3.2 Problems with aDNA-based approaches

Whilst aDNA has shed light on a number of key questions about the past, its analysis is not without difficulty. Assuming physiological conditions were maintained post-mortem, it would take up to 100,000 years for endogenous nucleases to completely digest DNA [19]. Furthermore, DNA inherently undergoes a number of changes over time which make intact sequences even more difficult to retrieve. Two main types of damage that occur are hydrolytic damage that deaminates the bases, and oxidative damage that causes modifications to bases [19]. This often results in the retrieval of only very small fragments of DNA as well as the incidental co-extraction of any low molecular weight compounds that are present in the environment where the sample is found [27, 28]. Often these small compounds are oxidised thymine and cytosine residues that impede the activity of DNA polymerase, and thus render PCR approaches ineffective [27].

The retrieval of aDNA is further complicated depending on the location of the specimen being sampled. For example, a plant or animal specimen stored in a museum, under optimum controlled conditions during both initial retrival and curation, may be easy to sample, and is compatible with PCR as is routinely used in such circumstances. Conversely, archaeological samples that are found *in situ* and are exposed to a wide range of both known and unknown environmental conditions over large periods of time may have very little to no DNA remaining which is suitable for analysis. This makes it difficult to discern the authenticity and validity of the ancient DNA, in the context of potential contamination from modern DNA [27, 28].

The problem of contamination with contemporaneous DNA is a major hurdle in the analysis of aDNA and can occur at any stage of the experiment such as excavation, storage, or even during DNA extraction. Another source of contamination is bacteria or fungi that exist on the ancient sample. The presence of microorganism or modern human DNA results in the contaminant DNA being amplified during PCR instead of the minimal amounts of aDNA can lead to false positives that raise questions about the authenticity and reproducibility of the experiment [27].

1.4 Ancient proteomics

The challenges associated with working with aDNA have resulted in researchers looking for alternative biomolecular approaches to studying ancient biological materials. With recent advances in proteomic analyses and technologies, proteins have become the new frontier within bioarchaeology. Mass spectrometry (MS) has become a powerful tool in the analysis of ancient proteins in archaeological remains [1, 8, 29]. The analysis of these robust biomolecules has revealed significant information relevant to our understanding of both history and science.

1.4.1 Advantages of proteins over DNA

Proteins represent the functional components of the genome, in that they are what the DNA encodes for after transcription and translation. Proteins, unlike DNA, cannot be amplified but are fortunately found in high abundance, representing a substantial component of all tissues in a living organism. This lack of amplification also decreases the likelihood of mistaking contamination for a true result [30]. These macromolecules are constructed from linear chains of amino acids, with the sequence of those reflecting the DNA that encodes the protein. Understanding this connection between coding DNA and protein sequences means that a protein identified in one species can be compared to the same protein in different species in order to discern the levels of relatedness between two organisms [30-32]. Identifying the protein profile of a sample through the use of high-throughput, high-resolution proteomic workflows allows for the identification of potential biomarkers or proteins of interest in a sample of archaeological remains that can, for example, indicate disease state at the time of death. Notable proteomic investigations of ancient human remains and other archaeological materials are discussed further below.

1.4.2 Proteomic analysis of 500-year-old Incan Mummies

Proteomic analysis is capable of detecting disease state at the time of death in human remains in a way that aDNA analysis is not able to. An excavation on the summit of Mount Llullaillaco in Argentina led to the discovery of three mummies, a seven-year-old boy, six-year-old girl, and a fifteen-year-old girl referred to as ‘the Maiden’ [3, 33]. The mummies were dated to the time of the Incan empire, approximately 500 years ago. Radiological and physical analysis of the Maiden revealed a series of pathologies consistent with multiple potential diseases, whilst the boy displayed no lesions, mucosal enlargement or signs of respiratory infection. Oral, buccal, and blood swabs in addition to a small piece of textile were collected

from the boy and the Maiden and analysed using a shotgun proteomics approach. The identified proteins in the Maiden sample revealed a high abundance of immune response proteins consistent with pulmonary bacterial infection, whilst the boy displayed normal levels of immune response proteins [3]. The etiological agent of the infection, hypothesized to be a species of *mycobacteria*, was identified using PCR of aDNA extracted from the Maiden, and was successfully verified as such. This study was capable of detecting active infection on a molecular level 500 years post-mortem and is an exemplar of the applicability of proteomics to archaeological and forensic sciences.

1.4.3 Proteomic analysis of 4200-year-old Egyptian Mummies

Another more recent example of identifying pathology in archaeological remains through the use of proteomics is the analysis of three Egyptian mummies. A shotgun proteomics workflow applying high-resolution nanoflow LC-MS/MS (nanoLC-MS/MS) was conducted on microsampled skin and muscle biopsies from three First Intermediate Period (~4200 years ago) Egyptian mummies [4]. This protocol resulted in the identification of 230 unique proteins in total, including both collagenous and non-collagenous proteins. Notable non-collagenous proteins identified include a high abundance of inflammation and immune response proteins such as myeloperoxidase, eosinophil peroxidase, cathepsin G, and proteinase 3. The abundance of these proteins preserved in the sample after such a length of time indicates that one of the mummies may have suffered from a potentially fatal bacterial pulmonary infection [4]. This study highlights the molecular-level information that can be generated via microsampling from archaeological materials, and how this data can be used to inform our understanding of human pathogens and immune responses.

1.4.4 Proteomic analysis of 2000-year-old Osteogenic Sarcoma

The analysis of pathologies present in archaeological remains can be used to inform modern medicine with regard to disease states. Osteosarcoma is a primary malignant tumour of the bone that commonly affects young adolescents and children. Due to metastases in tumour progression prior to clinical diagnosis, this form of cancer has poor prognosis [6]. A study into a 2000-year-old case of osteosarcoma evident in an archaeological bone sample from Hungary has led to further understanding of this disease. The bone, belonging to a female aged between 25 and 35, was analysed using a shotgun proteomics approach. Modern healthy humerus samples were collected as a control. The study discovered a number of upregulated proteins

that are potential tumour biomarkers including annexin A10, BCL-2, calgizzarin, HSP ß-6 protein, rho GTPase-activating protein 7, transferrin and vimentin. These proteins were identified in detectable quantities despite being sampled from a 2000-year-old bone, indicating they were most-likely over-expressed at the time of death, which may be suggestive of the cause of death in this individual [6].

1.4.5 Analysis of ancient bone collagen fingerprinting as radiocarbon screening and species identification tool

Collagen is one of the most abundant proteins in mammals and is present in the extracellular space in connective tissue as well as in bone and fibrous tissues such as tendons, skin, and ligaments [34-36]. Collagen fingerprinting is a high-throughput and low-cost analytical method that requires microsampling of bone collagen followed by tryptic digestion to generate peptide mass fingerprints (PMF), which are then analysed via soft ionisation mass spectrometry. The advantages of using collagen for PMF in bioarchaeology are that collagen is capable of large-scale survival due to how closely it associates with hydroxyapatite in bone and that collagen sequences have unique genus-level fingerprinting that allows for exogenous contaminants to be correctly identified [34-37].

In archaeology, radiocarbon analysis of collagen from bone samples is the most common method of dating, however it is expensive and difficult to screen samples for reliable date yields. Buckley and colleagues, in a 2016 study, developed a method of using collagen fingerprinting as a pre-screening tool for radiocarbon dating [34]. They found that extracted bone collagen samples which produced excellent collagen fingerprints also yielded good radiocarbon dates, whilst poor collagen fingerprint samples resulted in failed or inconclusive dating data. This study revolutionised the way in which radiocarbon dating is conducted with archaeological remains and highlights further applications of protein analysis in bioarchaeology.

Species identification is a vital part of archaeological research when dealing with large bone deposits, particularly in the case of livestock, animal husbandry, and hunting within ancient civilisations [35, 36]. This is made particularly difficult when the excavated bones lack clear morphological markers. An adapted method of collagen fingerprinting used in the case of animal bones is Zooarchaeology by Mass Spectrometry (ZooMS), which utilises the genus-specific fingerprint of collagen to differentiate between species [35, 36, 38, 39]. A ZooMS analysis of 32 different mammalian species with known domestic, livestock, or other

anthropogenic uses revealed 92 unique peptide markers with the potential to identify species [35]. This study revealed new ways proteomic data can be incorporated into bioarchaeology to determine individual species from bones, independent of morphology, and as a means of revealing contemporaneous contamination that may be introduced either during or post-excavation.

A further study of the applicability of ZooMS to archaeology was conducted on the identification of marine mammals such as pinnipeds and cetaceans [36]. Human interactions with coastal and marine environments have been vital to human survival and subsistence throughout our evolution. Interactions such as fishing have resulted in large quantities of skeletal remains occurring in the archaeological sites neighbouring coastlines. Marine mammal bones are difficult to visually identify and distinguish between species due to a lack of morphological features and characteristics. A collection of 54 archaeological bone specimens lacking key morphological discriminators, from seven different North Atlantic sites dating between the Mesolithic and Early Modern period (~10,000 BCE – 1500CE), were subject to ZooMS analysis [36]. This study was able to firstly identify collagen sequences in ancient samples of varying ages, and secondly to use these collagen sequences to differentiate between various cetacean and pinniped species. It was found that of the 54 samples, 26 were cetaceans including porpoises (*Phocoenidae*), sperm whales (*Physeter microcephalus*), and dolphins (*Delphininae*); and 25 were pinnipeds including earless seals (*Phocidae*) and walruses (*Odobenus rosmarus*). The remaining three samples were found to be bovine, possibly from animal husbandry that also occurred in the region [36]. This study highlights that collagen fingerprinting can provide molecular-level phylogenetic data that can be used to distinguish individual species within large archaeological bone deposits.

1.4.6 Proteomic analysis of an Iñupiat potsherd

Proteomic analysis can be applied to a range of archaeological materials, including those that are not inherently organic or biological. A study into a 1200-1400 CE Iñupiat potsherd from Point Barrow, Alaska revealed that proteins bind to the clay matrix of cooking vessels and are preserved over time [5]. This study presents a method to identify such proteins in order to identify the diet of previous Indigenous populations. A modern control was made by heating blubber and muscle tissues from three native species of seal (*Phoca vitulina*, *Halichoerus grypus*, and *Phoca hispida*) and beluga whale (*Delphinapterus leucas*) in a ceramic vessel to develop an extraction methodology for the ancient potsherd. Both the modern and ancient

ceramics were subject to liquid nitrogen grinding, solubilisation in trifluoroacetic acid, and in-solution digestion prior to analysis using MALDI-TOF mass spectrometry. The identification of cetacean and pinniped proteins in the ancient potsherd validates the oral tradition of seal hunting being a fundamental aspect of indigenous life in this region, and the role of such activities in diet [5]. The extraction of proteins from ceramics confirms the potential for proteomic analysis of art and inorganic, non-biological archaeological materials and the ability for scientific data to validate historical data.

1.4.7 Protein Deamidation as potential dating tool

Archaeological research is heavily dependent on the presence of robust absolute dating of cultures, sites, and artefacts. Radiometric dating, such as ^{14}C radioisotope dating, is perhaps the most well-known and extensively used method in the field today, but it is not without limitation [34]. A proposed novel complementary dating technique is the use of protein deamidation ratios to assess the relative age of samples [40, 41]. Proteins are known to undergo various chemical and structural modifications over time such as the deamidation of glutamine and asparagine residues into carboxylic acids. The deamidation of asparagine is known to have a half-life measurable on a physiological timescale (0.5 – 500 days in peptides) whereas the deamidation of glutamine is considerably slower (600 – 20,000 days) [41]. This makes it much more useful for the analysis and relative dating of archaeological materials.

An experimental software package, DeamiDATE, is currently being developed which can utilise MaxQuant output files to determine deamidation ratios and the relative age of both the given sample, and the individual proteins that were experimentally discovered. This was highlighted in the analysis of a skull from Whitehawk Camp, a Neolithic site located in Brighton, United Kingdom (~2700 BCE) [40]. Initial proteomic analysis of this skull revealed the presence of chicken egg proteins, despite chickens not being present in England until approximately 500BCE. By analysing the deamidation ratios of the chicken egg proteins against the human proteins in the same sample, the authors discovered that the chicken egg proteins were much ‘younger’ than the human proteins, but still older than modern contaminants and the trypsin used in sample preparation. They concluded that the egg proteins were resultant from restoration work performed in the mid-1900s during a time when animal-based glues were commonly used in curatorial spaces. The DeamiDATE software was able to distinguish between the individual protein deamidation ratios in this data to discern the age discrepancies between ancient proteins of different ages [40].

1.4.8 Sex estimation using amelogenin protein fragments

Sex estimation is a vital part of the bioarchaeological analysis of bones and human skeletal remains, particularly in regard to reconstructing population demographics, cultural dynamics, and the experience of health and disease. Presently, this is done through one of two methods, which are the analysis of sexually dimorphic bone features or the detection of DNA markers specific to the X- or Y-chromosomes [42]. The osteological approach is both non-destructive and efficient but is limited in the analysis of bones belonging to late adolescents and adults who can display sexually dimorphic bone structures resultant from hormonal or behavioural changes during and post-puberty. The alternative DNA method is much more costly and destructive but uses X- and Y-chromosome specific genes as molecular markers for sex estimation. The most prominently used marker is the amelogenin gene family which has been characterised to have X- and Y-specific isoforms (*AMELX* and *AMELY*). This approach is predicated on the preservation of the DNA molecule in the sample, which is heavily dependent on the age and environmental conditions of the sample, as described above (see §1.3).

Amelogenin is a protein produced in teeth that plays an intrinsic role in enamel development and biomineralisation [43]. It is known that biomineralised proteins are more likely to be preserved on a longer timescale, making the sex-linked protein isoforms of amelogenin a suitable alternative to DNA analysis for sex estimation in archaeology [37, 42, 44, 45]. A study of 40 enamel samples representing 25 individuals of different contexts, from modern samples to ancient adult and deciduous teeth dating up to approximately 7300 years old, used shotgun LC-MS/MS to detect amelogenin peptides. AMELX was discovered in varying signal strengths in all samples, but AMELY was found in only 26 samples from 13 individuals. Samples with AMELY were unambiguously male, whilst the samples without AMELY could be either low-signal male false negatives or female samples [42]. This study demonstrates protein-based signals can be reliably detected from ancient and relatively poorly preserved samples for sex estimation.

1.5 Paleoproteomics and phylogeny

Paleoproteomics is defined as the study of proteins present in fossilised materials. It utilises high-throughput, high-resolution analytical methodologies to generate molecular-level

phylogenetic information through the identification of protein sequences that remain preserved in fossils [37, 45-51].

1.5.1 Soft-tissue preservation in fossilised remains

It has long been believed that the process of fossilisation results in the complete destruction of organic material, and that the original molecular components of an organism will be lost or modified to undetectable amounts over a relatively small timeframe (less than a million years) [49, 50]. However, this has come under scrutiny with the discovery of intact structures present in fossils and has led to a very controversial series of studies into soft-tissue preservation and fossil proteins [37, 45, 49-54]. In a 2007 study, Schweitzer and colleagues reported the discovery of soft tissue structures in demineralised samples of *Tyrannosaurus Rex* skull, vertebrae, femora and tibiae. They theorised that the presence of soft-tissue remnants is indicative of the survival of proteins such as collagen, which is known to associate closely with the hydroxyapatite structure of bone. Furthermore, molecular analyses were conducted on these samples using enzyme-linked immunosorbent assay (ELISA) and time-of-flight secondary ion mass spectrometry (TOF-SIMS). Antibody binding reactions were confirmed using *in situ* immunohistochemistry which revealed antibodies against collagen had bound to the demineralised material. TOF-SIMS analysis was able to identify the amino acid sequence in the protein fragments to generate a molecular phylogeny based on sequence similarities which suggested birds descended from dinosaurs based on sequence similarities [50].

According to Schweitzer, a likely theory as to how proteins are preserved over such large stretches of time is due to the decay of red blood cells in an organism post-mortem releasing metals such as iron which then interact with proteins. This interaction links proteins together and causes them to precipitate out of solution where they dry out in a way that facilitates preservation [44, 45]. Another theory is the role of biomineralization of collagen with hydroxyapatite after death. Most collagens and keratins are not biomineralized in life, however they are negatively charged molecules and thus may associate with minerals present in the burial environment, contributing to ongoing stability of the macromolecule long after the death of the organism [45].

1.5.2 Proteomic analysis of *Tyrannosaurus Rex* femur

Proteomic analysis relies on the generation of spectral information such as mass to charge ratios of peptides and fragments, which are converted into peptide information through cross-

referencing with genome sequences and corresponding protein sequence data. When this information is lacking, the analysis of proteins in a sample is significantly more cumbersome. Unknown peptide sequences identified using mass spectrometry can be confirmed by comparing to peptide sequences of known organisms. If there is a sequence similarity, it indicates that the fragmentation pattern of the unknown peptide would match the theoretical fragmentation pattern of the known peptide in the protein database, thus confirming protein identity. Using this principle, collagen was sequenced from ostrich (*Struthio camelus*) femur bone before the ostrich genome had been published [54]. The extracted proteins were analysed using LC-MS/MS. The fragmentation pattern of 87 identified tryptic peptides were compared with those belonging to related organisms such as chickens (*Gallus gallus*) where it was found that approximately 33% of collagen α1t1 and 16% of collagen α2t1 sequences were identified using this methodology. This approach was then applied to the analysis of collagen extracted from a 68 million-year-old *T. rex* femur specimen. Mass spectrometric data from this sample revealed a total of seven predicted collagen peptide sequences with fragmentation patterns similar to collagen α1t1, α2t1, or α1t2 from any extant vertebrate taxa in protein databases [54]. Advances in proteomic technologies and the preservation of soft tissue in fossils has allowed for the subsequent identification of proteins from several million-year-old dinosaur fossils. This study was initially criticised as the *T. rex* data were believed to be from modern contamination but is now considered to have marked the beginning of molecular phylogenetic studies in dinosaur evolution.

1.5.3 Analysis of unidentified Cretaceous Period therapod dinosaurs

Further study into soft-tissue preservation in the vertebrate fossil record has paved the way for more molecular analyses of dinosaur fossils. However, many of these studies have been conducted on samples which were considered exceptionally well preserved and had visible external indications of soft tissue. A collection of eight poorly preserved unidentified Cretaceous (~75 Million years ago) dinosaur bones with no discernible soft tissue preservation or morphological characteristics were analysed using scanning electron microscopy (SEM) and TOF-SIMS [47]. In one bone sample, structures resembling endogenous collagen fibre remains were observed which indicates the possible preservation of proteins. The TOF-SIMS analysis identified amino acid fragments consistent with collagen fibrils, although not enough was preserved to identify the species [47]. This study revealed that proteins may still be present in

fossil remains regardless of the overall state of preservation, but likely not in quantities sufficient for molecular phylogenetics, collagen fingerprinting, or species identification.

1.5.4 Proteomic analysis of Mammoth and Mastodon collagen sequences in bones and fossils

Proboscidean species represent a rich fossil record with a distinct morphology and a collection of diverse families including the Deinotheriidae, Mammutidae, Gomphotheriidae, Stegodontidae, and Elephantidae [39]. Despite this diversity only one family exists today; the Elephantidae, which includes two genera, *Elephas* in Asia, and *Loxodonta* in Africa. In order to confirm phylogeny and develop divergence relationships between the extinct and extant species, collagen fingerprinting was conducted on bone specimens from extinct species including mammoths (*Mammathus trogontherii* and *Mammathus primigenius*), the American mastodon (*Mammut americanum*), the straight-tusked elephant (*Palaeoloxodon antiquus*), and two extant species (*Elephas maximus* and *Loxodonta Africana*) [39]. The ages of the extinct specimens ranged from 10,000-years-old to 650,000-years-old, whilst the extant samples were from modern specimens. The study compared two LC-coupled ionisation techniques, matrix-assisted laser desorption/ionisation (MALDI) and electrospray ionisation (ESI), to assess their effectiveness in peptide identification in paleoproteomics. Bone powder was collected from each sample and demineralised for analysis using LC-MALDI and LC-ESI. It was found that in modern samples, there was no notable difference between the two ionisation techniques; however, LC-ESI produced significantly greater sequence coverage and peptide mass fingerprinting than LC-MALDI. This optimised technique and generated phylogenetic library was applied to the identification of two suspected mammoth bones from the British Middle Pleistocene (781,000 – 126,000 years ago) deposits in Eastern England. These bones were identified as Steppe mammoths (*M. trogontherii*), a species that derived from a similar ancestor to the modern Elephantidae [39].

1.6 Non-invasive analysis of archaeological materials

Most methods of scientific archaeological analysis are destructive and require invasive sampling or sample preparation, which is a significant concern for museums and cultural heritage conservationists [9, 14]. A number of non-invasive methods, including X-ray imaging and computed tomography (CT), have been applied to the study of archaeological materials to

generate a wealth of information that can inform our understanding of the past without compromising the integrity of the materials [55-57].

The application of X-ray radiography to archaeology has revolutionised the way in which artefacts and human remains are analysed and has allowed for greater integration of non-invasive analysis [56, 57]. Another radiographic technology used in archaeology, albeit to a lesser extent, is CT scanning, which has been instrumental to the investigation of novel technologies and complexities of production and consumption in ancient civilisations [57]. A study into Late Archaic American Southeast pottery (3000 – 1000 BCE) utilised CT scanning to identify 'micro-techniques' present in morphological characteristics in the ceramic fabric from various pottery production methods such as coiling, rolling, and casting [57]. This data was collected and used to establish a library of structural fingerprints for further typological analysis. This method was then applied to a series of ceramics retrieved from two neighbouring contemporaneous archaeological sites to construct a model of production methods, trade, and geographically-centred technological advances between communities in the region [57].

The scientific analysis of cultural heritage objects such as paintings and frescoes is an important area of research in archaeological science as it can elucidate information about the materials used [58, 59]. Despite the detailed information that can be generated from analysing these artefacts, the destructive component of their sampling is a significant concern for heritage conservationists. In order to address this issue, Righetti and colleagues have recently developed a non-invasive, non-destructive method for sampling proteins and small molecules from artworks [59]. A functionalised ethyl-vinyl acetate film was produced and coated in strong cation/anion exchange and C_8 resins, which allowed it to interact with both proteins and other smaller molecules such as lipids and metabolites that may be present on the surface of an object. This film was applied to two 16th Century CE frescoes located in the Parella castle in Italy for *in situ* protein and small molecule extraction. Following elution from the film with ammonium acetate, the extracts were subject to liquid chromatography coupled with tandem mass spectrometry (LC-MS/MS). It was found that the pigment was made using carminic acid while the binding agent used in making the pigments was bovine milk indicated by the identification of bovine ß-casein and α-S1-casein. Despite the fact that the proprietary sampling film is not yet readily available, this study shows great potential for non-invasive *in situ* molecular sampling of paintings and artworks in bioarchaeological analyses, as well as the potential application of this method to sampling other materials.

1.6.1 Non-invasive sampling and bioarchaeology

One of the main aims of the research described in this thesis was to develop a non-invasive technique for sampling organic remains, using readily available equipment and materials. Our rationale is that a non-destructive sampling method would be much more palatable to museum curators, and hence would enable access to a much wider range of ancient materials. We set out to examine whether skin sampling strip tape as used in dermatology could be successfully applied to the analysis of ancient materials.

1.7 Skin sampling strips

The use of skin sampling strips is common practice in dermatology and has been predominantly used in the isolation of microorganisms from the *stratum corneum* and the identification of skin infections such as atopic dermatitis, psoriasis, and bacterial infections [60, 61]. In recent years, tape stripping methods have been applied to the extraction of biomolecules such as lipids and proteins [62, 63].

A study into the changes in lipid profile of surface layer skin in atopic dermatitis patients *versus* healthy patients used tape stripping methods to collect samples for the analysis. The stripping method was able to isolate short-chain ceramides and sphingolipids. It was discovered that the proportion of short-chain ceramides were increased while the proportion of the corresponding long-chain species were decreased indicating that type 2 immune activation in atopic dermatitis patients affects skin lipid metabolism when compared to healthy controls [62].

Surface layer skin protein expression profiles have been analysed in atopic dermatitis patients to potentially identify new disease biomarkers [63]. Tapes were applied to acute, chronic, and non-lesional instances of atopic dermatitis on the backs, arms, and legs of five patients and five healthy control patients. The extracted proteins were subject to MS analysis and the spectral counts of proteins of interest were quantified across sample groups. It was found that skin proteins such as dermicidin and cytoskeletal keratin type II were downregulated in acute and chronic atopic dermatitis cases, whilst serpin B3 and epidermal fatty acid binding proteins were upregulated. It is proposed that these protein expression changes are linked to skin inflammation and immune system responses. Furthermore, alpha-enolase was present exclusively in all atopic dermatitis samples which correlates with data from previous studies on psoriasis and the role of this protein in chronic inflammation [63, 64]. This study validated

the usefulness of tape strip application protocols in the non-invasive sampling for the proteomic analysis of skin.

During the course of this thesis, a paper was published which coupled sampling using skin sampling strips with high resolution mass spectrometry to perform a proteomic analysis of genetic defects present in autosomal recessive congenital ichthyosis (ARCI) [65]. This study extracted keratinocytes for proteomic analysis using sampling strips applied to patients suffering with ARCI gene mutations, including three subjects with *TGM1*, three with *SDR9C7*, and four with *PNPLA1* mutations, in addition to seven healthy controls. Extracted proteins were digested and peptides were analysed on a Thermo Scientific Q Exactive Plus Orbitrap mass spectrometer. This study was able to identify phenotypic manifestations related to the three selected ARCI-associated gene mutations using sampling strips, and discovered proteomic variabilities between individuals and also between sample sites within the same individual. The PNPLA1 gene mutation was found to be the most divergent form of ARCI in terms of proteomic alterations, with 138 proteins having a marked difference in expression compared to the other two genes and the controls. A total of 24 unique keratins were identified to have altered expression levels in this study, of which 19 were found to be downregulated in ARCI patients compared to control [65]. This study was the first to highlight the compatibility of sampling using dermatological grade sampling strips with high resolution mass spectrometry in the identification of proteins including, but not limited to, keratins and collagens.

1.8 Aims and scope of this thesis

Our initial aim was to develop a protocol for non-destructive sampling of the surface layer of modern skin, compatible with subsequent proteomic analysis using high resolution mass spectrometry. Our major aim, contingent on the success of the initial studies, was to adapt the protocol for application to the analysis of a series of available ancient Egyptian remains, and determine whether this would yield significant bioarchaeological information.

2 Methodology

2.1 Application of skin sampling strips to modern samples

Modern skin surfaces were used as a surrogate for the initial method development experiments. The anterior surface of the left forearm of a healthy volunteer was cleaned with 70% ethanol and wiped with a lint-free tissue prior to sampling. A D-Squame D100 skin sampling strip (22mm diameter, CuDerm Corporation, Texas, USA) was applied with 10 seconds of uniform pressure to the cleaned surface (see Figure 1). A total of 9 strips were then applied in succession to the site and pooled into groups of 1, 3, and 5 strips, respectively.

Figure 1 – Application of a D-Squame skin sampling strip to modern sample. Strip outlined in black marker on the anterior surface of the left forearm. Image: Author's own.

2.2 Mer-Neith-it-es Remains

This project is aimed at developing a novel minimally-invasive sampling technique for the proteomic analysis of bioarchaeological materials. *Modern skin surfaces were used as a surrogate for the initial method development experiments.* The ancient samples analysed in this thesis belong to a 26th Dynasty (ca. 664 - 525 BCE) Egyptian mummy named 'Mer-Neith-it-es', curated by the Nicholson Museum, University of Sydney. Acquired in the mid-19th Century by Sir Charles Nicholson, the coffin of Mer-Neith-it-es (NMR.29) was initially thought to be an empty cedar coffin [66]. CT imaging of the coffin in 2017, shown in Figure 2, revealed that it was, in fact, not empty and contained the disarticulated and highly fragmented remains of a

single unidentified mummified individual. The age at time of death, sex, and cause of death are unknown, but the remains are believed to be those of a female adult. The proof-of-concept work presented in this thesis was made possible by the poorly preserved condition of the remains.

Figure 2 – X-ray CT image of the burial coffin of Mer-Neith-it-es (Coffin NMR.29) prior to excavating contents. Image courtesy of Nicholson Museum, University of Sydney, NSW. CT scanning performed by Macquarie Medical Imaging, Macquarie University.

2.3 Application of skin sampling strips to ancient samples

Application of D-Squame skin sampling strips to a series of eight skull fragments and four other bone fragments from Mer-Neith-it-es was performed during a visit to the Nicholson Museum in March 2019, as shown in Figures 3 and 4 on the following pages. Sampling was performed on both the endo- and ectocranial surfaces of the skull fragments and the mandible (referred to hereafter as the interior and exterior surfaces), resulting in the 21 sets of sampling strips being collected. No cleaning was performed prior to sampling. The number of strips used across the bone surfaces was determined by fragment surface area, with 3 strips being applied to smaller fragments and 5 strips for larger fragments. The strips were collected into Eppendorf tubes and labelled with the museum accession number, specific surface location, and number of strips used.

Figure 3 (opposite) – Mer-Neith-it-es Bone fragment samples. Images: Author's own (A) Wrapped feet and tibia in storage container; (B) exposed surface of wrapped tibia sampled with D-squame skin sampling strips; (C) humeral shaft (approximately 18cm length); (D) molar; (E) mandible fragment (approximately 9cm length) .

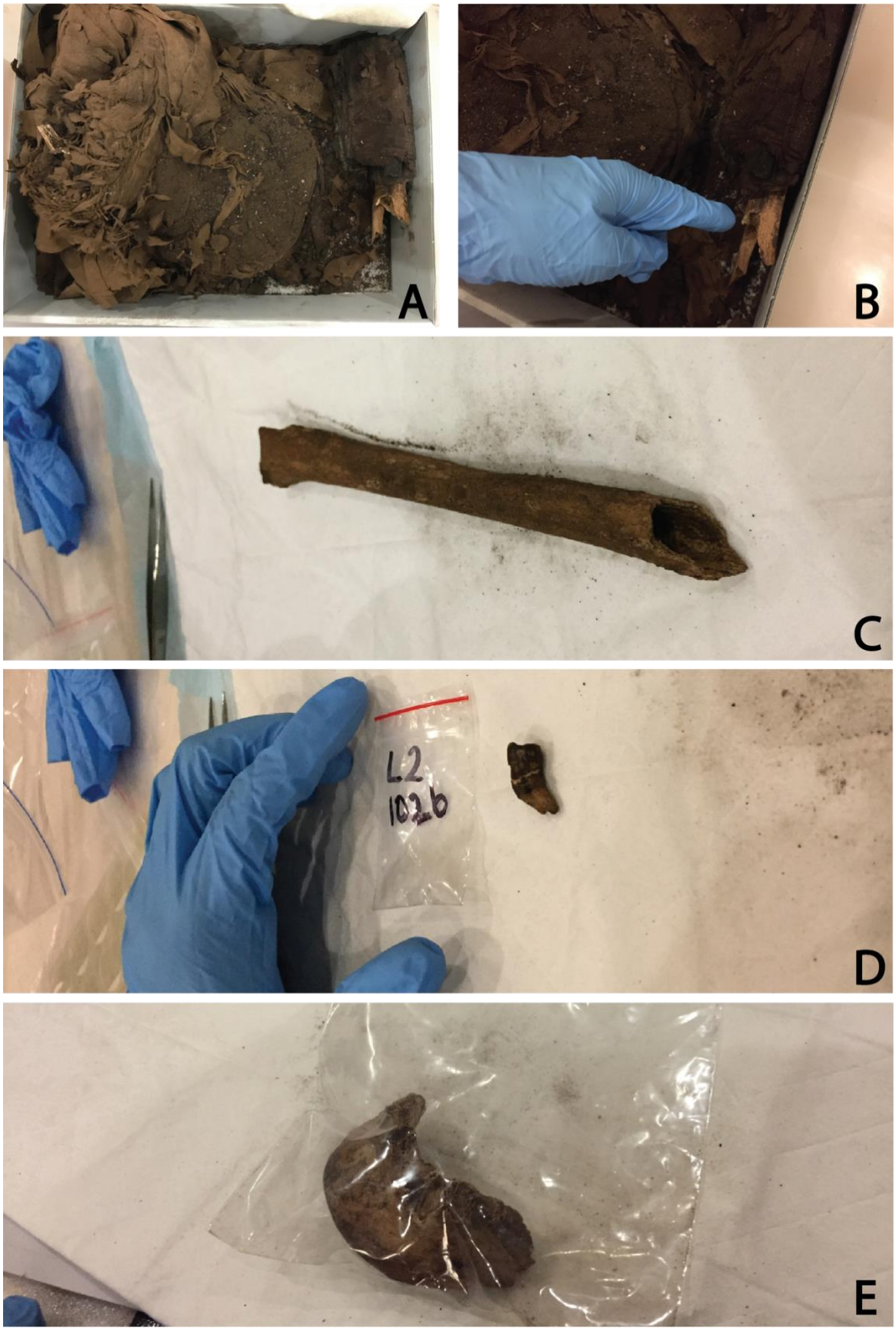
A
B
C
L2
102b
D
E

Figure 4 (opposite) – Mer-Neith-it-es Skull fragment samples. Images: Author's own. (A) skull fragment 1443; (B) skull fragment 559; (C) skull fragment 549; (D) skull fragment 1459; (E) skull fragment 1134; (F) skull fragment 1034; (G) application of D-Squame skin sampling strip to skull fragment 1439; (H) application of D-Squame skin sampling strip to skull fragment 1476. Scale bar in plates A-F is 8cm.

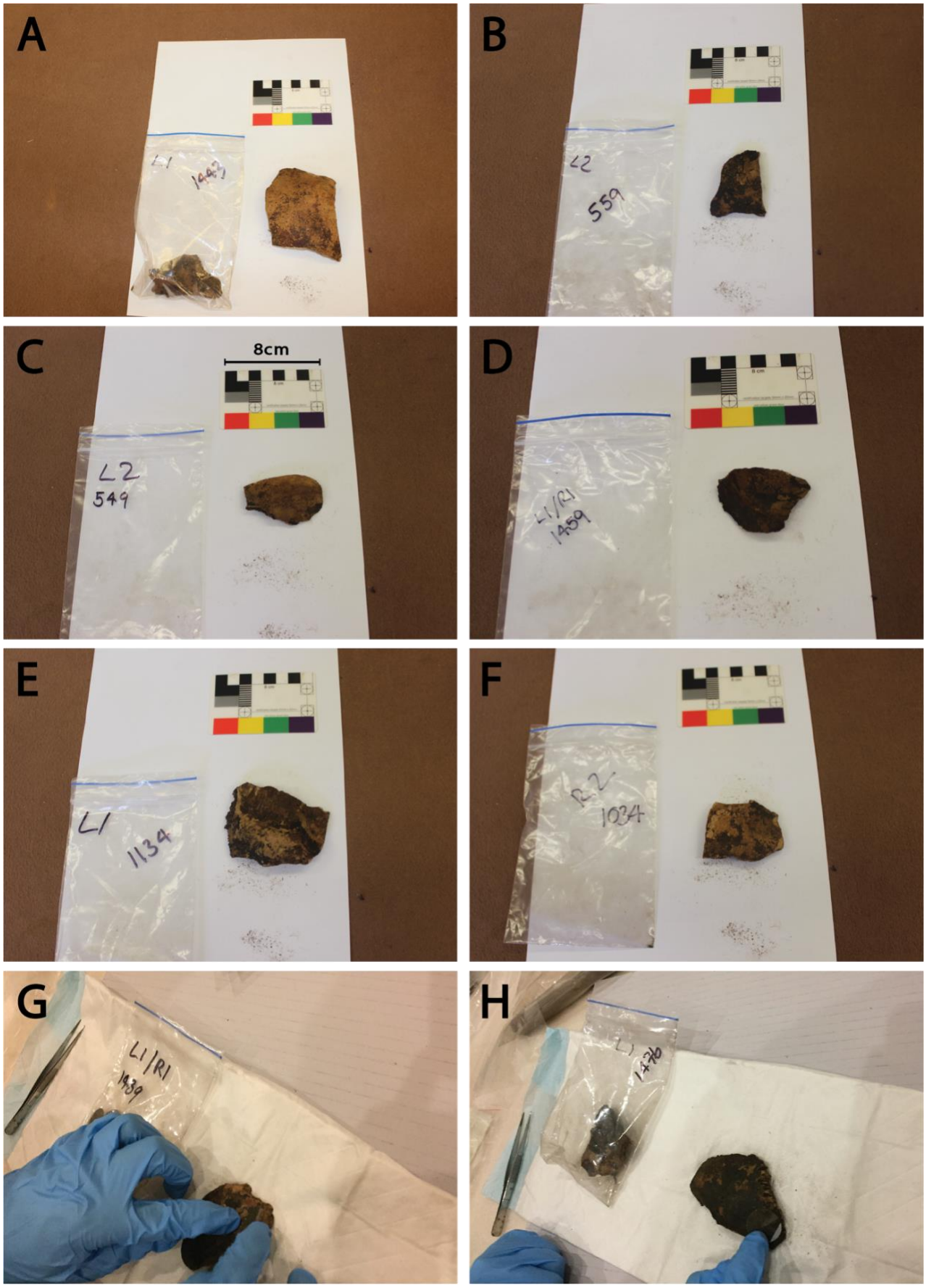
A
B
C
8cm
D
E
F
G
H

2.4 Extraction of proteins from skin sampling strips

Each strip or group of strips was transferred to a fresh 1.5mL Eppendorf tube with 1mL phosphate buffered saline (PBS) and bath sonicated for 15 minutes at room temperature [67]. The supernatant was transferred to a fresh 15mL falcon tube and 9 mL of ice-cold acetone was added. Proteins were precipitated at -20ºC for two hours before centrifugation at 13,000 rpm for 10 minutes. Supernatant was decanted and the protein pellet was left to air-dry briefly.

2.5 SDS-PAGE of strip extracts

The pellet was resuspended in 50 µL of 2x SDS (Sodium dodecyl sulfate) Loading Buffer (100mM Tris-Cl, 4% SDS, 0.2% bromophenol blue, 20% glycerol, 200mM dithiothreitol) then heated to 95ºC for exactly 5 minutes. Samples were run on a precast gel (Bio-Rad 10% Mini-PROTEAN® TGX™, 10 x 50 µL wells) alongside 30 µL of protein marker (Bio-Rad, Precision Plus Unstained Marker) at 100 V for an hour. The proteins were visualised using colloidal Coomassie blue staining and sample lanes were excised and divided into 8 equal fractions for further analysis.

2.6 Trypsin in-gel digestion

SDS-PAGE gel band fractions were finely chopped and transferred to 1.5mL Eppendorf tubes and washed briefly with 200µL of 100mM NH_4HCO_3 before destaining by washing three times with 200µL of 50% acetonitrile (ACN)/ 50mM NH_4HCO_3 for 10 minutes and dehydrating with 100% ACN. The samples were briefly left to air-dry and then reduced with 50µL of 10mM dithiothreitol (DTT) in 100mM NH_4HCO_3 at room temperature for 1 hour. DTT solution was removed and replaced with 55mM iodoacetamide (IAA) in 100mM NH_4HCO_3 and incubated in the dark at room temperature for 1 hour. Gel pieces were then washed once with 100µL of 100mM NH_4HCO_3 for 10 minutes, twice with 200µL of 50% ACN/ 50mM NH_4HCO_3, then dehydrated with 100% ACN and air-dried. Samples were then rehydrated with 30µL of 10ng/µL trypsin (Promega, Sequencing Grade Modified Trypsin) in 50mM NH_4HCO_3 at 4ºC for 30 minutes before overnight digestion at 37ºC. After digestion, peptides were extracted using 30µL of 50% ACN/ 2% formic acid (FA) (Mass Spectrometry grade, Fluka Analytical), then repeated twice more, once with 70% ACN/ 2% FA, then 90% ACN/ 2% FA. Extracts were then dried in a vacuum centrifuge and reconstituted in 10µL of 1% FA for nanoLC-MS/MS.

2.7 NanoLC-MS/MS of peptide extracts

Extracted peptides were analysed using a Thermo Q-Exactive orbitrap mass spectrometer coupled to a Thermo Easy-nLC1000 system. Reversed-phase chromatographic separation was conducted using a C18 HALO column (2.7µm bead size, 160Å pore size) of 75µm I.D. x 75mm. A linear gradient of 1-50% solvent B (99.9% ACN/0.1% FA) was run over 60 minutes. Data-dependent acquisition mode was configured to automatically switch from Orbitrap MS to MS/MS mode. Spectra were acquired from a m/z range of 350 to 1600 amu with a resolution of 35,000 and an isolation window of 3.0m/z. The ten most abundant ions were then selected for higher energy collisional dissociation (HCD) fragmentation at 30% normalised HCD collision energy, with dynamic exclusion of target ions was set for 20 seconds. Fragmentation ions were detected in the orbitrap at a resolution of 17,500.

2.8 Protein Identification using X! Tandem

Raw spectral files were converted to mzXML format and loaded into the Global Proteome Machine (GPM) software (version 3.0, available from https://www.thegpm.org/) using the X! Tandem algorithm. The files were searched against the SwissProt Human Protein database (downloaded January 2019; 20,329 proteins) and an in-built common Repository of Adventitious Proteins (cRAP) database which includes common lab contaminants and reagents. The search parameters were set as follows: Orbitrap method including ±20ppm parent mass tolerance, fragment mass tolerance of ±0.4Da, trypsin selected as digestion enzyme with up to two missed cleavages, fixed modification for carbamidomethylation of cysteine, and variable modifications including oxidation of methionine and tryptophan. Spectra were also searched against a reversed sequence database for evaluation of false discovery rates (FDR). Each of the 8 fractions of each sample were processed in sequential order then merged to generate an output file for each fraction and a merged sample file.

2.9 Calculating False Discovery Rate at Protein and Peptide level

The protein level FDR was calculated as a percentage from GPM output files where the *FDR = [(number of reversed protein identifications)/ (total number of protein identifications) * 100]*. Similarly, peptide level FDR was calculated as *FDR = [(number of reversed peptide identifications)/ (total number of peptide identifications) * 100]*. These calculations were performed for each sample across a range of log(e) values from -1 to -10 to assess the overall quality of the data and establish an appropriate stringency level for further bioinformatic

analysis, as shown in Figure 5. These calculations determined that applying a log(e) cut-off value of -3 to both the modern and ancient GPM outputs provided a peptide FDR range of 0% to 4.26% across the samples analysed, with an average peptide FDR of 0.64%, with the number of proteins identified in each sample ranging from 22 to 481.

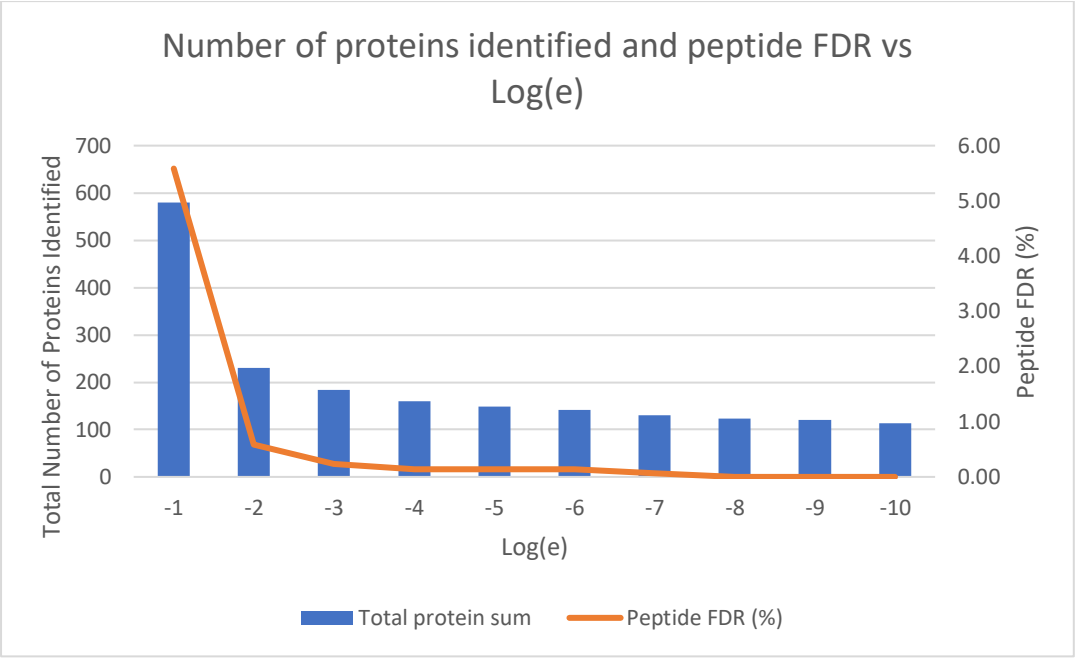

Figure 5 – Representative graph of stringency calculation process, displaying the number of total proteins identified and peptide FDR at each log(e) score from -1 to -10 for sample skull fragment 1439 interior. Graph shows that applying stringency values above log(e) -3 yields little to no significant decrease in peptide level FDR while minimising total amount of proteins.

2.10 Functional categorisation of identified proteins

Protein accession headers for each sample were extracted from the GPM output files and were categorised into biological function using GOTermMapper (https://go.princeton.edu/cgi-bin/GOTermMapper). Reversed sequence hits and common laboratory contaminants such as porcine trypsin, bovine serum albumin, and bovine ß-casein were excluded. Protein headers were entered into Basic Inputs and categorised using the following parameters: Ontology aspect was set to biological process, selected organism was *Homo sapiens* (GOA @EBI + Ensembl), and Ontology was set to Generic slim. Results were exported into a HTML table for further analysis. An enrichment calculation was performed on samples containing 50 or more identified proteins at the assigned log(e) cut-off by taking the GO term usage in gene list percentage and dividing it by the Genome frequency of use percentage.

3 Results and Discussion

3.1 Development of protein extraction protocol from skin sampling strips

The method development process involved applying D-Squame sampling strips to modern skin, then extracting proteins into solution for SDS-PAGE separation and subsequent trypsin in-gel digestion for nanoLC-MS/MS analysis. Extraction of proteins from the strips occurred in PBS with sonication. Due to time constraints and the initial success of this method in identifying modern proteins, it was applied to the subsequent analysis of the ancient samples presented in this thesis without any further attempt at method optimisation. SDS-PAGE was used primarily as a separation and desalting technique for strip extracts. The sample lanes of the gels were very faint and difficult to image effectively due to the relatively small amount of proteins within each sample. Lanes displayed a smear when visualised instead of distinct bands which is characteristic of degraded proteins, as shown in Figure 6 below. Similarly, the discolouration of the dye front ranged from green to brown, indicating the presence of humic substances in the samples [68].

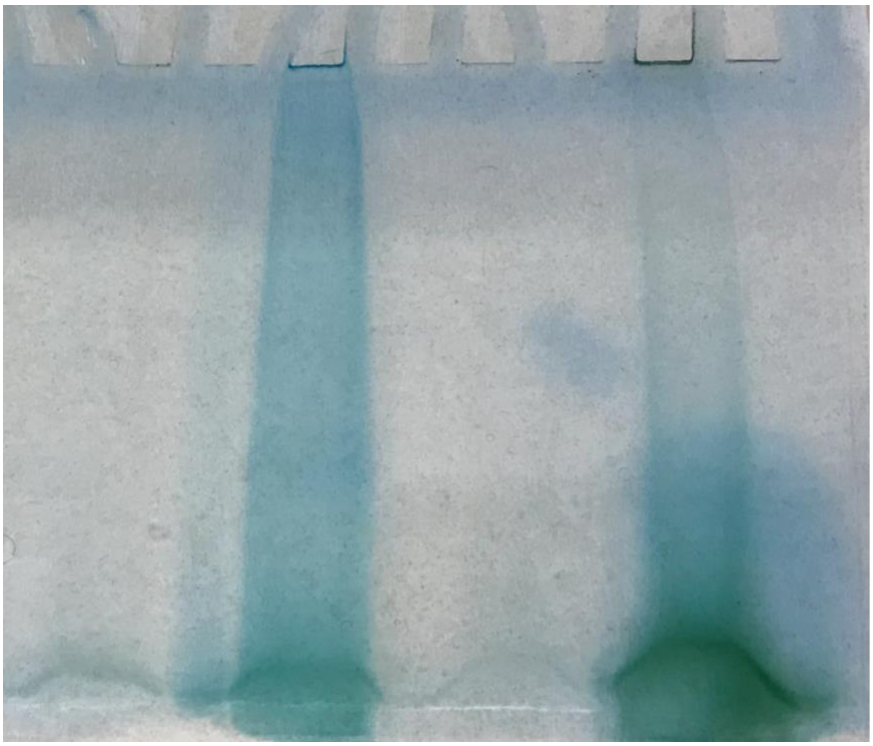

Figure 6 – Representative SDS-PAGE image of Mer-Neith-it-es sample indicating the smearing and discolouration of the dye front that occurred when running the ancient samples.

The overall protein identification from GPM and gene ontology (GO) data collected from all modern and ancient samples is summarised in Table 1 (overleaf). GO category terms listed in Table 1 represent biological processes that proteins identified in the corresponding sample are associated with. The number of protein and peptide identifications and the peptide FDR percentage were calculated at a protein log(e) cut-off value of -3.

3.1.1 Proteomic analysis of modern strip samples

The analysis of the modern skin strip samples represents the method development component of this thesis. As stated in §2.1 , the modern skin sampling involved the use of 9 strips which were then divided into groups of 1, 3, and 5 strips in order to test for correlation between the number of strips used and the number of proteins subsequently identified. The number of protein identifications were found to not correlate linerarly with the number of strips used in this experiment, as summarised in Table 1. While the 5 strip sample produced the most protein identifications, the 3 strip sample was found to have significantly fewer identifications than the 1 strip sample. This suggests there may be an issue with overcrowding of the strips in the Eppendorf tube during extraction. Initial experiments used larger tubes, but it was found that the strips migrated out of solution during sonication, and therefore subsequently yielded little to no proteins.

The types of proteins identified in the modern strip samples varied between the number of strips used. The 1 and 3 strip samples consisted mostly of keratins and other cytoskeletal proteins, while the 5 strip sample containing more immune system proteins such as immunoglobulins and serpins. This is likely an artefact of deeper skin layers being sampled by the sequential application of 5 strips to the same site. A blank control was also performed, consisting of 5 strips which were removed from the packaging and analysed without application to any surfaces and minimal exposure to lab environment. The 14 proteins identified in this control were mainly keratins, porcine trypsin, common lab contaminants such as bovine serum albumin, and small amounts of abundant cellular proteins such as heat shock proteins, tubulin, and actin.

Table 1 – Summary of protein and peptide identification and GO data from modern and ancient samples

Sample	# proteins	# peptides	Peptide FDR %	# strips applied	Most abundant GO categories [a]	Most enriched GO categories [a b]	Comments
Modern							
Blank control	14	243	0	5	N/A	N/A	Keratins, Trypsin, common lab contaminants
1 strip modern	149	3958	0	1	Anatomical Structure Development; Transport	Nitrogen Cycle Metabolic Process; Protein Folding	Keratins, actin, tubulin, heat shock proteins
3 strips modern	89	3414	0.15	3	Anatomical Structure Development; Transport	Cell Wall Organisation; Nitrogen Cycle Metabolic Process	Keratins, actin, tubulin, cytoskeletal proteins
5 strips modern	189	5158	0.15	5	Transport; Immune System Process	Cell Wall Organisation; Nitrogen Cycle Metabolic Process	Keratins, actin, tubulin, immunoglobulins, serpins, intracellular proteins
Ancient							
Humeral shaft	454	11221	0.23	9	Cellular Nitrogen Compound Metabolism; Transport	Protein Folding; Nitrogen Cycle Metabolic Process	Keratins, tubulin, actin, filamins, plectin, plastin, myosin
Tibia	84	904	0.19	5	Transport; Anatomical Structure Development	Cytoskeleton-dependent Intracellular Transport; Plasma Membrane Organisation	Tubulin, actin, cytoskeletal, membrane, and intracellular proteins
Mandible interior	93	892	0.1	3	Transport; Anatomical Structure Development	Cytoskeleton-dependent Intracellular Transport; Generation of Precursor Metabolites and Energy	Tubulin, actin, Central Nervous System-related proteins, keratins
Mandible exterior	25	104	0.48	3	Anatomical Structure Development; Cell Differentiation	N/A	Mostly keratin, some intracellular proteins
Molar	17	53	4.26	3	Anatomical Structure Development; Cytoskeletal Organisation	N/A	Collagen, keratins, tubulin, actin
Skull 1034 interior	47	711	0.43	3	Transport; Biosynthetic Process	N/A	Keratins, actin, intracellular proteins, brain proteins
Skull 1034 exterior	133	3022	0.38	3	Cellular Nitrogen Compound Metabolism; Biosynthetic Process	Protein Folding; Nucleobase-containing Compound Catabolic Process	Keratins, actin, tubulin, intracellular proteins, chaperones
Skull 1134 interior	86	1640	0.51	5	Transport; Anatomical Structure Development	Cytoskeleton-dependent Intracellular Transport; Protein Targeting	Keratins, actin, tubulin, some intracellular proteins
Skull 1134 exterior	94	2207	0.35	5	Cellular Nitrogen Compound Metabolism; Biosynthetic Process	Protein Folding; Ribonucleoprotein Complex Assembly	Keratins, actin, tubulin, Heat shock proteins, chaperones
Skull 1443 interior	210	3457	0.4	5	Cellular Nitrogen Compound Metabolism; Biosynthetic Process	Protein Targeting; Protein Folding	Keratins, actin, tubulin, neural-related proteins, brain proteins
Skull 1443 exterior	78	2337	0.93	5	Anatomical Structure Development; Signal Transduction; Cellular Nitrogen Compound Metabolism	Transposition; Cell Junction Organisation	Keratins, collagens, actin, tubulin, intracellular proteins
Skull 1459 interior	130	2740	0.32	3	Cellular Nitrogen Compound Metabolism; Biosynthetic Process	mRNA Processing; Protein Folding; Translation	Keratins, actin, tubulin, neural-related proteins, brain proteins
Skull 1459 exterior	22	478	0.33	3	Anatomical Structure Development; Cell Differentiation	N/A	Mainly keratins, some low peptide count intracellular proteins

Table 1 Continued

Skull 1439 interior	177	2727	0.23	3	Anatomical Structure Development; Cell Differentiation	Nitrogen Cycle Metabolic Process; Protein Folding	Keratins, actin, tubulin, neural-related proteins, extracellular matrix proteins
Skull 1439 exterior	120	784	1.06	3	Anatomical Structure Development; Transport	Protein Folding; Cytoskeleton-dependent Intracellular Transport; Generation of Precursor Metabolites and Energy	Keratins, actin, tubulin, neural-related proteins, some brain proteins
Skull 1476 interior	188	1801	2.09	5	Anatomical Structure Development; Cellular Nitrogen Compound Metabolism	Protein Folding; Ribonucleoprotein Complex Assembly; Translation	Keratins, actin, tubulin, neural-related proteins, intracellular proteins
Skull 1476 exterior	134	1431	1.68	5	Anatomical Structure Development; Transport	Protein Folding; Plasma Membrane Organisation	Keratins, actin, tubulin, some brain and neural-related proteins, intracellular proteins
Skull 549 interior	457	16851	0.34	3	Transport; Cellular Nitrogen Compound Metabolism	Protein Targeting; Protein Folding	Keratins, actin, tubulin, large number of brain and neural-related proteins
Skull 549 exterior	398	9788	0.2	3	Transport; Anatomical Structure Development	Protein Folding; Cytoskeleton-dependent Intracellular Transport; Nucleobase-containing Compound Catabolic Process	Keratins, actin, tubulin, large number of brain and neural-related proteins
Skull 559 interior	242	5568	0.43	3	Cellular Nitrogen Compound Metabolism; Transport	Nitrogen Cycle Metabolic Process; Protein Folding	Keratins, actin, tubulin, neural-related proteins, brain proteins, muscle proteins
Skull 559 exterior	292	11617	0.19	3	Anatomical Structure Development; Transport	Plasma Membrane Organisation; Protein Folding	Keratins, actin, tubulin, neural-related proteins, brain proteins, muscle proteins

[a] Top 3 categories recorded in table where percentage values between categories were equal or within 0.1 of each other.
[b] Enrichment calculations performed on samples containing 50 or more protein IDs at a log(e) cut-off of -3.

3.2 Protein identification of ancient bone samples

This section and the following §3.3 deal with the results from the proteomic analysis of the 21 sets of sampling strips applied to ancient bone and skull fragments; the samples explored in §3.2 are the humeral shaft, tibia, mandible interior and exterior, and molar. For samples with 50 or more protein identifications, the top 20 most abundant proteins based on redundant peptide counts are reported in Tables 2, 3, and 4 on the following pages.

3.2.1 Proteomic analysis of humeral shaft

A total of 454 proteins were identified from the humeral shaft strip samples, as summarised in Table 1, with the most abundant proteins reported in Table 2. These proteins include keratins and collagens as expected, but also various intracellular proteins such as haemoglobin subunits alpha, beta, and delta, plectin, and filamin-A, -B, and -C. Plectin is an abundant structural protein in the cytoskeleton of several cell types, including muscle and skin [69]. Filamins are known to act as anchoring proteins for adhering transmembrane proteins to the actin cytoskeleton. Filamin-A and -B are ubiquitous in the body, whilst filamin-C is muscle-

specific and vital for maintaining structural integrity of muscle fibers [70]. A number of brain and neural-related proteins were also identified on the humeral shaft, possibly due to the jumbled nature of the skull and bone fragments within the coffin. Sampling was performed using 9 strips due to the length of the bone. During extraction, these strips were divided into groups of 1, 3, and 5 strips, respectively, in an attempt to determine whether the number of strips used correlates linearly to the number of proteins identified via LC-MS/MS, similar to the modern strip extraction experiment in §3.1.1. Once again, no correlation was found as the 1 and 3 strip extracts produced a similar number of protein identifications of around 250 proteins at log(e) of -3, and the 5 strip had 64 identified proteins at the same cut-off. This further suggests that overcrowding of strips in the tubes prevents efficient protein extraction.

Table 2 – Top 20 most abundant proteins from humeral shaft sample

Identifier	# total peptides	log(e)	Description
K2C1_HUMAN	788	-442.4	Keratin, type II cytoskeletal 1
K1C10_HUMAN	490	-368.3	Keratin, type I cytoskeletal 10
TBA1B_HUMAN	384	-215.5	Tubulin alpha-1B chain
TBA1A_HUMAN	375	-213.2	Tubulin alpha-1A chain
TBA1C_HUMAN	312	-203.7	Tubulin alpha-1C chain
K22E_HUMAN	290	-303.7	Keratin, type II cytoskeletal 2 epidermal
TBA4A_HUMAN	279	-213.1	Tubulin alpha-4A chain
K1C9_HUMAN	255	-213.8	Keratin, type I cytoskeletal 9
TBA3C_HUMAN	254	-185	Tubulin alpha-3C/D chain
TBB4B_HUMAN	244	-282.1	Tubulin beta-4B chain
TBB2A_HUMAN	242	-283.5	Tubulin beta-2A chain
TBB4A_HUMAN	242	-246.5	Tubulin beta-4A chain
ACTG_HUMAN	225	-225.3	Actin, cytoplasmic 2
TBB5_HUMAN	223	-248.6	Tubulin beta chain
ACTB_HUMAN	220	-235.4	Actin, cytoplasmic 1
TBA8_HUMAN	205	-122.7	Tubulin alpha-8 chain
TBB3_HUMAN	144	-151.3	Tubulin beta-3 chain
FLNA_HUMAN	131	-375.5	Filamin-A
K2C6C_HUMAN	119	-154	Keratin, type II cytoskeletal 6C
MYH9_HUMAN	116	-327.7	Myosin-9

3.2.2 Proteomic analysis of exposed tibia

A total of three strips were applied to the exposed surface of the wrapped mummified tibia, resulting in 84 identified proteins consisting of mainly actins and tubulins in addition to intracellular proteins such as voltage-dependent anion-selective channel protein 1 (VDAC1), adenonsine triphosphate (ATP) synthase subunit alpha, and prohibitins (see Table 3). VDAC1 is a mitochrondrial outer membrane and plasma membrane protein, and is involved in apoptosis initiation by increasing mitochondrial permeability [71]. Many cellular processes are predicated on the availability and concentration of ATP within the cell; ATP synthase is a key enzyme which is responsible for the maintenance and regulation of ATP concentrations [72].

Studies into the molecular dynamics of this vital enzyme have discovered that subunit alpha is responsible for the fine-tuning of the rate of ATP hydrolysis [72]. Prohibitins, of which there are two family members, are proteins that have been credited with numerous functions such as cell cycle regulation, mitochondrial stress response, cell death, and senescence [73]. Glial fibrillary acidic protein (GFAP) and Creatine kinase B-type were also found on the tibia surface.

Table 3 – Top 20 most abundant proteins from exposed Tibia sample

Identifier	# total peptides	log(e)	Description
TBA1B_HUMAN	72	-165.4	Tubulin alpha-1B chain
TBA4A_HUMAN	66	-163.9	Tubulin alpha-4A chain
TBA1A_HUMAN	62	-162.1	Tubulin alpha-1A chain
TBB4B_HUMAN	56	-160.5	Tubulin beta-4B chain
TBB2A_HUMAN	55	-150.6	Tubulin beta-2A chain
TBB2B_HUMAN	54	-148	Tubulin beta-2B chain
TBB4A_HUMAN	53	-153.8	Tubulin beta-4A chain
TBA8_HUMAN	53	-115.8	Tubulin alpha-8 chain
TBB5_HUMAN	50	-149	Tubulin beta chain
TBB3_HUMAN	34	-95	Tubulin beta-3 chain
ACTG_HUMAN	33	-123	Actin, cytoplasmic 2
ACTB_HUMAN	29	-121.7	Actin, cytoplasmic 1
KCRB_HUMAN	20	-75.1	Creatine kinase B-type
TBB8_HUMAN	18	-56.5	Tubulin beta-8 chain
GFAP_HUMAN	16	-76.9	Glial fibrillary acidic protein
ATPA_HUMAN	15	-54.3	ATP synthase subunit alpha, mitochondrial
K1C10_HUMAN	15	-38.4	Keratin, type I cytoskeletal 10
VDAC1_HUMAN	12	-59.4	Voltage-dependent anion-selective channel protein 1
K2C1_HUMAN	10	-23.9	Keratin, type II cytoskeletal 1
POTEF_HUMAN	8	-42.5	POTE ankyrin domain family member F

3.2.3 Proteomic analysis of mandible interior

Analysis of the interior surface of the mandible resulted in the identification of 93 proteins, including tubulins and actins, as well as proteins related to neuron structure and the Central Nervous System (CNS) such as neurofilament light, medium, and heavy polypeptides, alpha-internexin, myelin proteolipid protein, and GFAP (see Table 4). These proteins are understood to have roles in the development, regulation, and function of the CNS observed in mice models [74]. The presence of these proteins on the interior surface of the mandible may indicate they are remnants from the mandibular nerve, which is the largest of the trigeminal nerves and is located in and around the lower jaw [75].

Table 4 – Top 20 most abundant proteins from mandible interior sample

Identifier	# total peptides	log(e)	Description
TBB4A_HUMAN	78	-200.3	Tubulin beta-4A chain
TBB4B_HUMAN	76	-179.8	Tubulin beta-4B chain
TBB5_HUMAN	73	-183.1	Tubulin beta chain
TBB2A_HUMAN	72	-173.9	Tubulin beta-2A chain
TBA1B_HUMAN	65	-150.5	Tubulin alpha-1B chain
TBA4A_HUMAN	64	-153.9	Tubulin alpha-4A chain
TBA1A_HUMAN	61	-149.2	Tubulin alpha-1A chain
TBB3_HUMAN	34	-122.4	Tubulin beta-3 chain
KCRB_HUMAN	31	-110.1	Creatine kinase B-type
NFL_HUMAN	27	-145	Neurofilament light polypeptide
ACTG_HUMAN	24	-100.1	Actin, cytoplasmic 2
NFM_HUMAN	22	-105.6	Neurofilament medium polypeptide
ACTB_HUMAN	22	-95.8	Actin, cytoplasmic 1
K2C1_HUMAN	20	-67.3	Keratin, type II cytoskeletal 1
AINX_HUMAN	13	-72.1	Alpha-internexin
ATPA_HUMAN	10	-53.1	ATP synthase subunit alpha, mitochondrial
ACTA_HUMAN	10	-36.1	Actin, aortic smooth muscle
GFAP_HUMAN	10	-26.2	Glial fibrillary acidic protein
CN37_HUMAN	9	-63	2-,3--cyclic-nucleotide 3--phosphodiesterase
K2C8_HUMAN	8	-9	Keratin, type II cytoskeletal 8

3.2.4 Proteomic analysis of mandible exterior

A total of 25 proteins were found on the exterior surface of the mandible, consisting mostly of keratins and actin. Of the 104 peptides identified in this sample, 86 belong to keratins, actins, and tubulins. Other identified proteins were mainly related to anatomical structure including cofilin-1 and filamin-A.

3.2.5 Proteomic analysis of molar

A total of 17 proteins were identified from the molar samples. These proteins were mainly keratins, tubulins, actin, and collagen. No proteins were identified that were specific to teeth. As summarised in Table 1, the peptide FDR for the molar was 4.26% which is considerably higher than the ideal value of <1%. This sample was reported at this FDR as the same log(e) cut-off value was applied to all samples for consistency. The high peptide FDR is a consequence of the relatively small number of proteins and peptides present in the dataset for this sample.

3.3 Proteomic analysis of ancient skull fragment samples

Section 3.3 deals with the results from the ancient skull fragments. These 16 samples are the result of applying sampling strips to the endo- and ectocranial surfaces of skull fragments

from the Mer-Neith-it-es remains identified as numbers 1034, 1134, 1443, 1459, 1439, 1476, 549, and 559 (see Figure 4). For samples with 50 or more protein identifications, the top 20 most abundant proteins based on redundant peptide counts are reported in tables 5 to 18 on the following pages.

3.3.1 Skull fragment 1034 interior

A total of 47 proteins were identified on the interior surface of skull fragment 1034, including a number of keratins and actins, but also a number of intracellular and brain related proteins such as mucin-19 and teneurin-3. Mucin-19 is known as ocular mucin, and is reported to be involved in the homeostasis of ocular mucus [76]. It is expressed in human cornea, conjunctiva, and lacrimal glands, and its presence on this fragment could be indicative of its location in the structure of Mer-Neith-it-es' skull, since the morphology of this skull fragment suggests that it may be part of an eye socket. Teneurin-3 is a brain protein responsible for the assembly of topographic circuits in the hippocampal region of the brain. The hippocampus is located towards the centre of the brain, and is responsible for our capacity for memory and spatial awareness [77].

3.3.2 Skull fragment 1034 exterior

A total of 133 proteins were found on the exterior surface of fragment 1034, with more keratins, actins, and tubulins than were identified on the interior surface of the same fragment. In addition to this marked difference, there were a number of intracellular proteins that were identified including a number of molecular chaperones such as heat shock proteins and various T-complex protein 1 subunits. GO analysis of this sample revealed that protein folding was the most enriched functional category. The T-complex protein-1 ring complex (TRiC) is a cytosolic chaperonin which has been shown to have neuroprotective functions in axonal transport in Huntington's disease cases [78]. It is currently unknown if this function of TRiC on axonal transport is present in wild-type neurons, but it has been observed to facilitate telomere maintenance by folding the telomerase cofactor TCAB1 [79].

Table 5 – Top 20 most abundant proteins from 1034 exterior sample

Identifier	# total peptides	log(e)	Description
K2C1_HUMAN	380	-222.2	Keratin, type II cytoskeletal 1
ACTG_HUMAN	207	-123.1	Actin, cytoplasmic 2
ACTB_HUMAN	174	-123	Actin, cytoplasmic 1
K1C9_HUMAN	127	-138.2	Keratin, type I cytoskeletal 9
K1C10_HUMAN	122	-179.4	Keratin, type I cytoskeletal 10

Table 5 Continued

TBA1B_HUMAN	99	-94.9	Tubulin alpha-1B chain
HS90B_HUMAN	76	-108.1	Heat shock protein HSP 90-beta
HS71A_HUMAN	67	-88	Heat shock 70 kDa protein 1A
HSP7C_HUMAN	65	-73	Heat shock cognate 71 kDa protein
ENOA_HUMAN	63	-98.4	Alpha-enolase
TBB5_HUMAN	54	-83.6	Tubulin beta chain
H2B1B_HUMAN	53	-15.2	Histone H2B type 1-B
HS90A_HUMAN	51	-60.1	Heat shock protein HSP 90-alpha
HSP72_HUMAN	48	-56	Heat shock-related 70 kDa protein 2
ACTA_HUMAN	43	-40.9	Actin, aortic smooth muscle
K22E_HUMAN	41	-94.9	Keratin, type II cytoskeletal 2 epidermal
CH60_HUMAN	38	-63.9	60 kDa heat shock protein, mitochondrial
ACTBL_HUMAN	38	-26.2	Beta-actin-like protein 2
TBB4B_HUMAN	36	-74	Tubulin beta-4B chain
EF1A1_HUMAN	36	-29.2	Elongation factor 1-alpha 1

3.3.3 Skull fragment 1134 interior

A total of 86 proteins were identified on the fragment 1134 interior surface, 37 of which were keratins, tubulins, or actins. A number of intracellular proteins were also identified in this sample but with fewer peptide counts; These include synapsin-1, liprin-α1, and ubiquitin thioesterase. Synapsin-1 is a neural phosphoprotein which coats synaptic vesicles, binds to actin cytoskeletal filaments, and is believed to play a role in neurotransmitter release [80]. Liprin-α1 is a scaffold protein identified to be an important regulator for integrin-mediated cell motility, as well as interacting with many proteins of largely uncharacterised functions, particularly in tumour cell lines [81]. Ubiquitin thioesterase is a hydrolase known to play an important regulatory role in protein turnover processes by preventing degradation through the removal of 'Lys-48'-linked conjugated ubiquitin. The poly-ubiquitination of Lys-48 in protein sequences is often referred to as the 'molecular kiss of death' due to its role in tagging proteins for proteasome degradation [82].

Table 6 – Top 20 most abundant proteins from 1134 interior sample

Identifier	# total peptides	log(e)	Description
K2C1_HUMAN	193	-145	Keratin, type II cytoskeletal 1
K1M1_SHEEP	146	-142.8	Keratin, type I microfibrillar 48 kDa, component 8C-1
KT33A_HUMAN	112	-83.2	Keratin, type I cuticular Ha3-I
KT33B_HUMAN	105	-66.2	Keratin, type I cuticular Ha3-II
K1M2_SHEEP	104	-123.3	Keratin, type I microfibrillar, 47.6 kDa
ALBU_HUMAN	91	-24.5	Serum albumin
K2M2_SHEEP	74	-161.9	Keratin, type II microfibrillar, component 7C
K1C10_HUMAN	63	-124.2	Keratin, type I cytoskeletal 10
ACTG_HUMAN	62	-54.3	Actin, cytoplasmic 2
ACTB_HUMAN	49	-53.9	Actin, cytoplasmic 1
K2M3_SHEEP	47	-111.5	Keratin, type II microfibrillar, component 5

Table 6 Continued

KRT35_HUMAN	40	-36.7	Keratin, type I cuticular Ha5
K22E_HUMAN	35	-83.3	Keratin, type II cytoskeletal 2 epidermal
TBA1A_HUMAN	31	-50.4	Tubulin alpha-1A chain
K1C9_HUMAN	29	-75.3	Keratin, type I cytoskeletal 9
K1H2_HUMAN	29	-15.7	Keratin, type I cuticular Ha2
KRT86_HUMAN	23	-71.7	Keratin, type II cuticular Hb6
KRHB1_HUMAN	21	-75.1	Keratin, type II cuticular Hb1
RS8_HUMAN	21	-35	40S ribosomal protein S8
KRT83_HUMAN	19	-75.3	Keratin, type I cuticular Hb3

3.3.4 Skull fragment 1134 exterior

A total of 94 proteins were identified on the exterior surface of skull fragment 1134. A number of intracellular proteins were identified, including serpin H1, peptidyl-prolyl cis-trans isomerase A (PPIA), and nucleophosmin. These proteins are all known to be involved in processes involving protein-protein interactions within the cell such as protein targeting, folding, or post-translational modification. Serpin H1 is a collagen-specific binding protein reported to have chaperone-like activity in the biosynthesis of collagen and collagen fibrils [83]. PPIA catalyses the cis-trans isomerisation of proline peptide bonds in protein backbones, which facilitates protein folding by accelerating the rate at which it occurs [84]. Nucleophosmin is a histone chaperonin which is known to be involved in several cellular processes including ribosome biogenesis, protein folding, tumour suppression, and signal transduction [85].

Table 7 – Top 20 most abundant proteins from 1134 exterior sample

Identifier	# total peptides	log(e)	Description
K2C1_HUMAN	339	-263.4	Keratin, type II cytoskeletal 1
ACTG_HUMAN	167	-93.4	Actin, cytoplasmic 2
K1C10_HUMAN	159	-207	Keratin, type I cytoskeletal 10
ACTB_HUMAN	142	-93.1	Actin, cytoplasmic 1
K1C9_HUMAN	121	-106.2	Keratin, type I cytoskeletal 9
H2B1C_HUMAN	88	-43.3	Histone H2B type 1-C/E/F/G/I
H2B1M_HUMAN	87	-37.5	Histone H2B type 1-M
K22E_HUMAN	77	-113.3	Keratin, type II cytoskeletal 2 epidermal
TBA1B_HUMAN	43	-43.4	Tubulin alpha-1B chain
PPIA_HUMAN	43	-22.1	Peptidyl-prolyl cis-trans isomerase A
ACTA_HUMAN	42	-45.2	Actin, aortic smooth muscle
K2C6C_HUMAN	39	-61.3	Keratin, type II cytoskeletal 6C
ENOA_HUMAN	33	-46.4	Alpha-enolase
K2C5_HUMAN	31	-68	Keratin, type II cytoskeletal 5
TBB5_HUMAN	25	-31.9	Tubulin beta-5 chain
HS90B_HUMAN	25	-31.2	Heat shock protein HSP 90-beta
CH60_HUMAN	19	-60	60 kDa heat shock protein, mitochondrial
TBB3_HUMAN	18	-26.3	Tubulin beta-3 chain
ACTBL_HUMAN	18	-13.8	Beta-actin-like protein 2
HS71A_HUMAN	16	-41.4	Heat shock 70 kDa protein 1A

3.3.5 Skull fragment 1443 interior

A total of 210 proteins were identified on the interior of skull fragment 1443. These include keratins, actins, and tubulins, as well as cofilin-1, glutathione-S-transferase P1, and POTE ankyrin domain family members F and I. Cofilin-1 is a non-muscle specific actin binding protein known to maintain and regulate actin cytoskeletal dynamics, playing an important role in cell morphology during mitosis and cytokinesis [86]. Glutathione-S-transferase P1 is a known negative regulator of cyclin-dependent kinase-5 in brain and neuronal cells, and its increased abundance in these cells has been linked to protection from neurodegenerative diseases such as Alzheimer's disease [87]. The POTE family proteins are ATP-binding proteins believed to play a role in retinal homeostasis based on their detection in tears [88]. PPIA, GFAP, and mucin-19 were also identified in this sample.

Table 8 – Top 20 most abundant proteins from 1443 interior sample

Identifier	# total peptides	log(e)	Description
K2C1_HUMAN	343	-277.1	Keratin, type II cytoskeletal 1
ACTG_HUMAN	262	-206	Actin, cytoplasmic 2
ACTB_HUMAN	250	-208.9	Actin, cytoplasmic 1
K1C10_HUMAN	239	-282.7	Keratin, type I cytoskeletal 10
K1C9_HUMAN	127	-140.2	Keratin, type I cytoskeletal 9
K22E_HUMAN	100	-186.4	Keratin, type II cytoskeletal 2 epidermal
PPIA_HUMAN	83	-83.8	Peptidyl-prolyl cis-trans isomerase A
ACTA_HUMAN	60	-87.3	Actin, aortic smooth muscle
K2C6B_HUMAN	59	-93.8	Keratin, type II cytoskeletal 6B
POTEF_HUMAN	55	-65.9	POTE ankyrin domain family member F
G3P_HUMAN	49	-115.5	Glyceraldehyde-3-phosphate dehydrogenase
K1C14_HUMAN	45	-82.8	Keratin, type I cytoskeletal 14
H2B1B_HUMAN	43	-9.1	Histone H2B type 1-B
K1C16_HUMAN	40	-78.6	Keratin, type I cytoskeletal 16
ACTBL_HUMAN	37	-41.1	Beta-actin-like protein 2
K2C8_HUMAN	37	-36.7	Keratin, type II cytoskeletal 8
K2C6A_HUMAN	33	-91.2	Keratin, type II cytoskeletal 6A
K2C7_HUMAN	32	-13.8	Keratin, type II cytoskeletal 7
GFAP_HUMAN	31	-8.3	Glial fibrillary acidic protein
K2C80_HUMAN	31	-8.1	Keratin, type II cytoskeletal 80

3.3.6 Skull fragment 1443 exterior

A total of 78 proteins were identified on the exterior surface of fragment 1443, including a number of keratins, collagens, actin, and tubulin. Other proteins identified include neutrophil defensin-1, hornerin, and endoplasmic reticulum chaperon BIP. Neutrophil defensin-1 is an antimicrobial peptide known to be involved in immune system responses within the body, particularly the innate immune response of mucosa in the nasal passage, trachea, lungs, and colon [89, 90]. Hornerin is an epidermal protein that comprises the envelope of cornified cells

and assists in the development of a skin barrier [91]. Endoplasmic reticulum chaperon BIP is a protein localised in the endoplasmic reticulum lumen that is involved in correct protein folding and subsequent degradation of misfolded proteins, and has also been reported to have heat shock protein-like activity in stressed cell states [92].

Table 9 – Top 20 most abundant proteins from 1443 exterior sample

Identifier	# total peptides	log(e)	Description
K1C10_HUMAN	314	-310.5	Keratin, type I cytoskeletal 10
K2C1_HUMAN	252	-347.3	Keratin, type II cytoskeletal 1
K22E_HUMAN	162	-300.6	Keratin, type II cytoskeletal 2 epidermal
K1C9_HUMAN	136	-250	Keratin, type I cytoskeletal 9
ACTG_HUMAN	113	-100.4	Actin, cytoplasmic 2
CO1A2_HUMAN	105	-158.5	Collagen alpha-2(I) chain
ACTB_HUMAN	87	-97.6	Actin, cytoplasmic 1
CO1A1_HUMAN	56	-143.4	Collagen alpha-1(I) chain
K2C6B_HUMAN	41	-38.7	Keratin, type II cytoskeletal 6B
K1C14_HUMAN	36	-76.7	Keratin, type I cytoskeletal 14
K1C16_HUMAN	25	-45.4	Keratin, type I cytoskeletal 16
PPIA_HUMAN	22	-8.3	Peptidyl-prolyl cis-trans isomerase A
K2C5_HUMAN	21	-63.6	Keratin, type II cytoskeletal 5
ALBU_HUMAN	20	-20.8	Serum albumin
H2B1B_HUMAN	17	-8.5	Histone H2B type 1-B
DEF1_HUMAN	14	-10.5	Neutrophil defensin 1
BBS2_HUMAN	14	-7.9	Bardet-Biedl syndrome 2 protein
NPM_HUMAN	13	-31.3	Nucleophosmin
TBA1A_HUMAN	13	-26.4	Tubulin alpha-1A chain
ENOA_HUMAN	12	-37.7	Alpha-enolase

3.3.7 Skull fragment 1459 interior

A total of 130 proteins were identified on the interior surface of fragment 1459, including keratins, actin, and tubulin. A number of proteins related to mRNA processing and translation were also identified including various elongation, transcription, and eukaryotic initiation factors, as well as proteins such as nucleolin, and 40S ribosomal proteins S3a, SA, and S3. Nucleolin is a nucleolar protein in growing eukaryotic cells, and is believed to play a role in pre-rRNA transcription and ribosomal assembly, in addition to transcriptional elongation [93]. Translation and mRNA processing, along with protein folding, were found to be enriched in the GO term analysis of this sample, as shown in Table 1.

Table 10 – Top 20 most abundant proteins from 1459 interior sample

Identifier	# total peptides	log(e)	Description
K2C1_HUMAN	280	-284.1	Keratin, type II cytoskeletal 1
ACTG_HUMAN	275	-225.6	Actin, cytoplasmic 2
K1C10_HUMAN	246	-293.1	Keratin, type I cytoskeletal 10
ACTB_HUMAN	236	-220.7	Actin, cytoplasmic 1

Table 10 Continued

K22E_HUMAN	122	-223.3	Keratin, type II cytoskeletal 2 epidermal
TBA1A_HUMAN	107	-127	Tubulin alpha-1A chain
TBA1C_HUMAN	83	-92.6	Tubulin alpha-1C chain
K1C9_HUMAN	80	-153.9	Keratin, type I cytoskeletal 9
ACTC_HUMAN	70	-92.3	Actin, alpha cardiac muscle 1
ACTA_HUMAN	69	-91.8	Actin, aortic smooth muscle
POTEF_HUMAN	68	-63.2	POTE ankyrin domain family member F
ACTBL_HUMAN	55	-71.2	Beta-actin-like protein 2
TBB2B_HUMAN	54	-80.8	Tubulin beta-2B chain
TBB5_HUMAN	53	-72.7	Tubulin beta chain
TBB3_HUMAN	50	-62.2	Tubulin beta-3 chain
K2C6A_HUMAN	39	-114.1	Keratin, type II cytoskeletal 6A
H2B1B_HUMAN	37	-14.3	Histone H2B type 1-B
K2C4_HUMAN	35	-75	Keratin, type II cytoskeletal 4
TBB4B_HUMAN	35	-70.9	Tubulin beta-4B chain
K1C16_HUMAN	32	-66.7	Keratin, type I cytoskeletal 16

3.3.8 Skull fragment 1459 exterior

Analysis of the exterior of skull fragment 1459 resulted in the identification of 22 proteins, of which 13 were keratins. Keratins were the most abundant protein by peptide count in this sample. A few intracellular proteins, such as pyruvate carboxylase and protocadherin gamma-C5, were identified with low peptide counts.

3.3.9 Skull fragment 1439 interior

A total of 177 proteins were identified on the interior surface of skull fragment 1439. These include keratins, actin, and tubulin, as well as neural-related proteins including neurofilament polypeptides and alpha-internexin. Membrane-binding proteins such as desmoplakin and annexin A2 were also identified. Alpha-internexin is a self-assembling neuronal intermediate filament protein involved in the morphogenesis of neurons and the postsynaptic actin cytoskeleton, and is believed to form independent structural networks without other neurofilament involvement [94]. Desmoplakin is a major component of desmosomes and is involved in the organisation and linkage of desmosomal cadherin-plakoglobin complexes in plasma membranes [95]. Annexin A2 is a calcium-regulated membrane-binding protein which binds calcium ions with high affinity, and is known to link protein complexes to the actin cytoskeleton [96].

Table 11 – Top 20 most abundant proteins from 1439 interior sample

Identifier	# total peptides	log(e)	Description
K1C10_HUMAN	358	-422.5	Keratin, type I cytoskeletal 10
K2C1_HUMAN	230	-359.9	Keratin, type II cytoskeletal 1
K2C6A_HUMAN	79	-271.1	Keratin, type II cytoskeletal 6A
K2C6B_HUMAN	77	-258.3	Keratin, type II cytoskeletal 6B
K1C17_HUMAN	69	-211.8	Keratin, type I cytoskeletal 17
ACTB_HUMAN	54	-102.4	Actin, cytoplasmic 1
ACTG_HUMAN	52	-106.2	Actin, cytoplasmic 2
TBA1B_HUMAN	51	-105.4	Tubulin alpha-1B chain
NFL_HUMAN	48	-168.7	Neurofilament light polypeptide
TBA4A_HUMAN	41	-83.8	Tubulin alpha-4A chain
K2C5_HUMAN	39	-201.9	Keratin, type II cytoskeletal 5
K1C9_HUMAN	37	-94.7	Keratin, type I cytoskeletal 9
K1H1_HUMAN	33	-162.5	Keratin, type I cuticular Ha1
K1C14_HUMAN	33	-142.1	Keratin, type I cytoskeletal 14
K22E_HUMAN	32	-150.5	Keratin, type II cytoskeletal 2 epidermal
KPRP_HUMAN	29	-138.8	Keratinocyte proline-rich protein
KT33B_HUMAN	28	-125.3	Keratin, type I cuticular Ha3-II
KRT86_HUMAN	26	-156.9	Keratin, type II cuticular Hb6
DESP_HUMAN	25	-164.6	Desmoplakin
KRT85_HUMAN	23	-142.3	Keratin, type II cuticular Hb5

3.3.10 Skull fragment 1439 exterior

A total of 120 proteins were identified on the exterior surface of fragment 1439, including keratins, actins, and tubulins. Other proteins identified include alpha-crystallin B chain, myelin basic protein, and haemoglobin subunit beta. Alpha-crystallin B chain is a small heat shock-like protein which contributes to the reflective index of the eye lens and has been reported to be a neuroprotective factor in mammalian retinal neurons [97]. Myelin basic protein is the most abundant protein component of myelin membranes and is believed to play a role in the myelination process of nerves in the CNS [98]. A number of brain and neural-related proteins such as neurofilament polypeptides, alpha-internexin, teneurin-3 and creatine kinase B-type were also found on this exterior skull surface.

Table 12 – Top 20 most abundant proteins from 1439 exterior sample

Identifier	# total peptides	log(e)	Description
K2C1_HUMAN	78	-200	Keratin, type II cytoskeletal 1
ACTG_HUMAN	53	-116	Actin, cytoplasmic 2
K1C9_HUMAN	51	-190.9	Keratin, type I cytoskeletal 9
ACTB_HUMAN	51	-117.2	Actin, cytoplasmic 1
K1C10_HUMAN	44	-116.9	Keratin, type I cytoskeletal 10
K22E_HUMAN	26	-113.1	Keratin, type II cytoskeletal 2 epidermal
TBA1A_HUMAN	21	-44.2	Tubulin alpha-1A chain
H2B1B_HUMAN	20	-24.2	Histone H2B type 1-B
NFL_HUMAN	16	-53.1	Neurofilament light polypeptide
NPM_HUMAN	14	-51.4	Nucleophosmin

Table 12 Continued

CRYAB_HUMAN	13	-58.5	Alpha-crystallin B chain
MBP_HUMAN	13	-42	Myelin basic protein
K1M1_SHEEP	12	-39.9	Keratin, type I microfibrillar 48 kDa, component 8C-1
ATPB_HUMAN	12	-17.3	ATP synthase subunit beta, mitochondrial
K2M2_SHEEP	8	-48.8	Keratin, type II microfibrillar, component 7C
1433B_HUMAN	8	-31.9	14-3-3 protein beta/alpha
K1M2_SHEEP	8	-27.2	Keratin, type I microfibrillar, 47.6 kDa
KCRB_HUMAN	8	-27.2	Creatine kinase B-type
K2C5_HUMAN	7	-40.6	Keratin, type II cytoskeletal 5
K2C6A_HUMAN	7	-25	Keratin, type II cytoskeletal 6A

3.3.11 Skull fragment 1476 interior

A total of 188 proteins were identified on the interior surface of fragment 1476, including keratins, actins, and tubulins. Other proteins identified include vimentin, transketolase, and pyruvate kinase. Vimentin is an RNA-binding protein that comprises the filaments found in non-epithelial cells such as mesenchymal cells [99]. Transketolase is an enzyme responsible for catalysing the transfer of two-carbon ketol groups from a ketose to an aldose in the pentose phosphate pathway [100]. Pyruvate kinase is a glycolytic enzyme that catalyses the production of ATP through the transfer of a phosphoryl group to adenosine diphosphate (ADP). It has also been reported to play a role in the caspase independent cell death of tumour cells [101]. Overexpression of these proteins has been reported as potential biomarkers for cancers and other disease such as congenital heart defects [6, 100, 101]. The fact that we are still able to detect these proteins approximately 2500 years after the time of death suggests that they may have been present at higher than normal levels at the time of death.

Table 13 – Top 20 most abundant proteins from 1476 interior sample

Identifier	# total peptides	log(e)	Description
K2C1_HUMAN	171	-279.2	Keratin, type II cytoskeletal 1
TBA1B_HUMAN	77	-109.7	Tubulin alpha-1B chain
TBA1A_HUMAN	73	-100.3	Tubulin alpha-1A chain
TBA1C_HUMAN	70	-94.9	Tubulin alpha-1C chain
K1C10_HUMAN	64	-198.1	Keratin, type I cytoskeletal 10
K22E_HUMAN	60	-206.3	Keratin, type II cytoskeletal 2 epidermal
K1C9_HUMAN	45	-117.9	Keratin, type I cytoskeletal 9
TBA4A_HUMAN	41	-95.8	Tubulin alpha-4A chain
ACTG_HUMAN	40	-100.7	Actin, cytoplasmic 2
ATPA_HUMAN	40	-54.6	ATP synthase subunit alpha, mitochondrial
ACTB_HUMAN	33	-97.9	Actin, cytoplasmic 1
TBB5_HUMAN	28	-70.5	Tubulin beta chain
HS90B_HUMAN	25	-96	Heat shock protein HSP 90-beta
TBB4B_HUMAN	25	-68.5	Tubulin beta-4B chain
K2C6A_HUMAN	24	-61.8	Keratin, type II cytoskeletal 6A
ENOA_HUMAN	23	-104.5	Alpha-enolase

Table 13 Continued

M4A10_HUMAN	23	-8.2	Membrane-spanning 4-domains subfamily A member 10
CH60_HUMAN	22	-112.7	60 kDa heat shock protein, mitochondrial
ATPB_HUMAN	22	-46.7	ATP synthase subunit beta, mitochondrial
TBB4A_HUMAN	21	-68.5	Tubulin beta-4A chain

3.3.12 Skull fragment 1476 exterior

A total of 134 proteins were identified on the exterior surface of fragment 1476. These include keratins, actins and tubulins as well as proteins such as clathrin heavy chain 1, dynamin-1, and hexokinase-1. Clathrin heavy chain 1 is a component of the trimeric protein clathrin, which plays a major role in the coating of coated pits and vesicles, the stability and function of mitotic spindles, and has been known to be involved in early autophagy processes [102, 103]. Dynamin-1 is a neuron-specific microtubule-associated enzyme involved in the production of microtubule bundles. It is capable of binding and hydrolysing guanosine triphosphate (GTP), and is required for efficient receptor-mediated endocytosis [104]. Hexokinase-1 is an enzyme which catalyses the phosphorylation of various hexoses within the body. This protein has also been observed to have innate immune and inflammation response activity by acting as a receptor for bacterial peptidoglycans [105].

Table 14 – Top 20 most abundant proteins from 1476 exterior sample

Identifier	# total peptides	log(e)	Description
K2C1_HUMAN	182	-287.7	Keratin, type II cytoskeletal 1
K1C10_HUMAN	78	-195.3	Keratin, type I cytoskeletal 10
TBA1B_HUMAN	77	-143	Tubulin alpha-1B chain
TBA1A_HUMAN	70	-131.6	Tubulin alpha-1A chain
K1C9_HUMAN	60	-116.7	Keratin, type I cytoskeletal 9
K22E_HUMAN	55	-205.5	Keratin, type II cytoskeletal 2 epidermal
TBA4A_HUMAN	44	-111.6	Tubulin alpha-4A chain
ACTG_HUMAN	32	-86.3	Actin, cytoplasmic 2
CLH1_HUMAN	31	-160.7	Clathrin heavy chain 1
ACTB_HUMAN	27	-89.1	Actin, cytoplasmic 1
ATPA_HUMAN	27	-17.8	ATP synthase subunit alpha, mitochondrial
DYN1_HUMAN	24	-133.7	Dynamin-1
TBB5_HUMAN	24	-87.3	Tubulin beta chain
TBB4B_HUMAN	24	-82.5	Tubulin beta-4B chain
CH60_HUMAN	22	-75.5	60 kDa heat shock protein, mitochondrial
TBB2A_HUMAN	22	-74.5	Tubulin beta-2A chain
TBB4A_HUMAN	20	-66	Tubulin beta-4A chain
K1C14_HUMAN	20	-52.6	Keratin, type I cytoskeletal 14
HXK1_HUMAN	18	-93.2	Hexokinase-1
HS90B_HUMAN	18	-48.2	Heat shock protein HSP 90-beta

3.3.13 Skull fragment 549 interior

A total of 457 proteins were identified on the interior surface of fragment 549, including the expected keratins, actins, and tubulins. A large number of proteins identified were brain or neural-related including creatine kinase B-type, syntaxin-binding protein 1, and septin-7. Creatine kinase B-type is an enzyme which catalyses the reversible transfer of phosphate groups from ATP to other phosphogens. It is expressed in high abundance in the brain, particularly in the right hemisphere of the cerebellum, and is known to play a role in the development of this region [106]. Syntaxin-binding protein 1 is an essential neurotransmitter protein and binds with syntaxin to form part of the synaptic vesicle fusion machinery [107]. Septin-7 is a cytoskeletal GTPase which closely associates with the actin cytoskeleton and is required for mitotic processes. This particular member of the septin protein family is highly expressed in the corpus callosum region of the brain [108]. Other notable proteins identified include GFAP, neurofilament polypeptides, synapsin-1 and -2, vimentin, pyruvate kinase, and various neuronal growth regulators.

Table 15 – Top 20 most abundant proteins from 549 interior sample

Identifier	# total peptides	log(e)	Description
TBB4A_HUMAN	768	-405.1	Tubulin beta-4A chain
TBA1B_HUMAN	713	-268.8	Tubulin alpha-1B chain
TBB4B_HUMAN	708	-364.1	Tubulin beta-4B chain
TBB2A_HUMAN	666	-381.2	Tubulin beta-2A chain
TBA1A_HUMAN	657	-263.6	Tubulin alpha-1A chain
K2C1_HUMAN	655	-513.1	Keratin, type II cytoskeletal 1
TBB2B_HUMAN	653	-365.1	Tubulin beta-2B chain
TBB5_HUMAN	615	-359.7	Tubulin beta chain
TBA4A_HUMAN	580	-251.7	Tubulin alpha-4A chain
TBA1C_HUMAN	526	-228.7	Tubulin alpha-1C chain
ACTG_HUMAN	455	-311.4	Actin, cytoplasmic 2
ACTB_HUMAN	444	-311.8	Actin, cytoplasmic 1
TBA8_HUMAN	411	-156.2	Tubulin alpha-8 chain
KCRB_HUMAN	378	-301.4	Creatine kinase B-type
K1C10_HUMAN	375	-416	Keratin, type I cytoskeletal 10
NFL_HUMAN	366	-476.4	Neurofilament light polypeptide
TBB6_HUMAN	300	-186.2	Tubulin beta-6 chain
TBB3_HUMAN	271	-265.1	Tubulin beta-3 chain
POTEE_HUMAN	265	-123.5	POTE ankyrin domain family member E
K22E_HUMAN	257	-442.6	Keratin, type II cytoskeletal 2 epidermal

3.3.14 Skull fragment 549 exterior

A total of 398 proteins were identified on the exterior surface of skull fragment 549. These include tubulins, keratins, actins, alpha-crystallin B-chain, and other proteins including contactin-1, spectrin alpha-II chain, and 2',3'-cyclic-nucleotide 3'-phosphodiesterase (CNPD).

Contactin-1 is a membrane protein responsible for cell adhesion in neuronal cell lines, with reported involvement in the formation of axons in the developing CNS [109]. Spectrin alpha-II chain is a non-erythrocytic member of the cytoskeletal spectrin protein family, and is known to be involved in axon organisation in the brain [110]. The exact function of CNPD in vertebrates is unknown, however it is known to bind RNA and cyclic nucleotide molecules and is the third most abundant protein in CNS myelin [111]. These proteins are all abundantly expressed in the brain, and expressed in lower frequencies in neuronal cells [109-111]. The detection of these abundant brain proteins on the exterior surface of the skull fragment is likely resultant from the delocalisation of the skeletal remains in the coffin.

Table 16 – Top 20 most abundant proteins from 549 exterior sample

Identifier	# total peptides	log(e)	Description
TBA1B_HUMAN	484	-228.1	Tubulin alpha-1B chain
TBA1A_HUMAN	443	-220.5	Tubulin alpha-1A chain
TBA1C_HUMAN	428	-199.2	Tubulin alpha-1C chain
K2C1_HUMAN	420	-430.2	Keratin, type II cytoskeletal 1
TBB4B_HUMAN	335	-208.5	Tubulin beta-4B chain
TBA4A_HUMAN	330	-189	Tubulin alpha-4A chain
TBB2A_HUMAN	312	-191.3	Tubulin beta-2A chain
TBB4A_HUMAN	306	-228.9	Tubulin beta-4A chain
TBB5_HUMAN	300	-207.2	Tubulin beta chain
TBA3C_HUMAN	276	-170.6	Tubulin alpha-3C/D chain
TBA8_HUMAN	243	-114.2	Tubulin alpha-8 chain
K1C10_HUMAN	207	-287.7	Keratin, type I cytoskeletal 10
K1C9_HUMAN	189	-236.1	Keratin, type I cytoskeletal 9
K22E_HUMAN	169	-296.8	Keratin, type II cytoskeletal 2 epidermal
MBP_HUMAN	165	-107.1	Myelin basic protein
TBB3_HUMAN	159	-110.8	Tubulin beta-3 chain
CH60_HUMAN	152	-235.8	60 kDa heat shock protein, mitochondrial
CRYAB_HUMAN	152	-155.7	Alpha-crystallin B chain
NFM_HUMAN	142	-231.4	Neurofilament medium polypeptide
ACTG_HUMAN	139	-168.1	Actin, cytoplasmic 2

3.3.15 Skull fragment 559 interior

A total of 242 proteins were identified on the interior surface of fragment 559, including several keratins, actins, and tubulins. Notable protein identifications include myosin-9, endoplasmin, and neuroblast differentiation-associated protein. Myosin-9 is a non-muscle variant of the myosin motor protein family. It is believed to play a crucial role in cell spreading during cytoskeletal reorganisation and in lamellipodial retraction [112]. Endoplasmin is a protein with reported heat shock protein-like and post-translational modification activity. It has been observed to interact with cofilin phosphatase chronophin in neuronal cells to mediate the formation of cofilin/actin rods [113]. Neuroblast differentiation-associated protein is an S100-

binding protein reported to facilitate the differentiation of neuronal cells in the developing CNS. It is highly expressed in the olfactory bulb located in the forebrain, but is also present in all neuronal cells [114].

Table 17 – Top 20 most abundant proteins from 559 interior sample

Identifier	# total peptides	log(e)	Description
K2C1_HUMAN	778	-491.1	Keratin, type II cytoskeletal 1
K1C9_HUMAN	452	-363.3	Keratin, type I cytoskeletal 9
K1C10_HUMAN	242	-300.3	Keratin, type I cytoskeletal 10
K22E_HUMAN	153	-267.5	Keratin, type II cytoskeletal 2 epidermal
K2C6B_HUMAN	106	-211.5	Keratin, type II cytoskeletal 6B
K2C6C_HUMAN	98	-228.9	Keratin, type II cytoskeletal 6C
K1C16_HUMAN	95	-216.8	Keratin, type I cytoskeletal 16
K2C6A_HUMAN	91	-227.9	Keratin, type II cytoskeletal 6ACK-6D
FLNA_HUMAN	87	-336.8	Filamin-A
K1C14_HUMAN	83	-176.3	Keratin, type I cytoskeletal 14
TBA1B_HUMAN	74	-116.8	Tubulin alpha-1B chain
K2C5_HUMAN	72	-163.4	Keratin, type II cytoskeletal 5
TBA1A_HUMAN	66	-106.1	Tubulin alpha-1A chain
CH60_HUMAN	64	-176.6	60 kDa heat shock protein, mitochondrial
TBA1C_HUMAN	62	-101.6	Tubulin alpha-1C chain
ENOA_HUMAN	60	-152.8	Alpha-enolase
M4A10_HUMAN	59	-8.4	Membrane-spanning 4-domains subfamily A member 10
KPYM_HUMAN	57	-137.2	Pyruvate kinase
TBB5_HUMAN	47	-136.3	Tubulin beta chain
ACTN4_HUMAN	45	-122.7	Alpha-actinin-4

3.3.16 Skull fragment 559 exterior

The analysis of the exterior surface of skull fragment 559 resulted in the identification of 292 proteins, including a number of tubulins, actins and keratins, as well as various 14-3-3 family proteins, glyceraldehyde-3-phosphate dehydrogenase (GAPDH), and phosphoglycerate mutase-1. The 14-3-3 protein family is a class of adapter proteins that are involved in the regulation of many signalling pathways throughout the body, particularly those in the brain, heart, and skeletal muscle [115]. GAPDH is an enzyme involved in the beginning stages of the pyruvate synthesis pathway, and has a number of reported functions including immune response, glycolysis, defense response, microtubule cytoskeleton organisation, and protein stabilisation [116]. Phosphoglycerate mutase-1 is a catalytic enzyme that interconverts 3- and 2-phosphoglycerate with 2,3-bisphosphoglycerate, and is believed to have protein kinase binding activity in the liver and brain [117].

Table 18 – Top 20 most abundant proteins from 559 exterior sample

Identifier	# total peptides	log(e)	Description
TBA1B_HUMAN	809	-302.6	Tubulin alpha-1B chain
TBA1A_HUMAN	765	-289.3	Tubulin alpha-1A chain
TBB4A_HUMAN	654	-311.7	Tubulin beta-4A chain
TBA4A_HUMAN	627	-284.5	Tubulin alpha-4A chain
TBB4B_HUMAN	602	-290.9	Tubulin beta-4B chain
TBB2A_HUMAN	582	-289.3	Tubulin beta-2A chain
TBB2B_HUMAN	569	-276.2	Tubulin beta-2B chain
TBB5_HUMAN	533	-285.7	Tubulin beta chain
TBA8_HUMAN	430	-175.6	Tubulin alpha-8 chain
TBA3E_HUMAN	418	-169.7	Tubulin alpha-3E chain
KCRB_HUMAN	374	-223.9	Creatine kinase B-type
ACTG_HUMAN	341	-215.4	Actin, cytoplasmic 2
ACTB_HUMAN	319	-213.4	Actin, cytoplasmic 1
TBB3_HUMAN	298	-210.3	Tubulin beta-3 chain
K2C1_HUMAN	269	-384.5	Keratin, type II cytoskeletal 1
TBB8_HUMAN	217	-102.1	Tubulin beta-8 chain
K1C10_HUMAN	173	-242.7	Keratin, type I cytoskeletal 10
K22E_HUMAN	140	-289.3	Keratin, type II cytoskeletal 2 epidermal
K1C9_HUMAN	128	-161.8	Keratin, type I cytoskeletal 9
ACTA_HUMAN	109	-96.3	Actin, aortic smooth muscle

3.4 Overall summary of protein identifications from all ancient skull and bone samples

There is some degree of variability present in both the number and types of proteins identified in each sample. It was found that the use of more strips did not necessarily equate to an increased number of protein identifications. Samples such as the mandible exterior, molar, skull 1034 interior, and skull 1459 exterior yielded few proteins (<50 identifications), indicating that either the strips were not always effective at collecting proteins from the sample surface, the extraction protocol used was not efficient, or simply there was little proteinaceous material left on the bone surface.

On average, the exterior surfaces of the skull fragments were more enriched for keratins while the interior surfaces were more enriched for intracellular, brain, and neural-related proteins. The higher abundance of keratins on the exterior surfaces is likely due to the presence of protein remnants from hair and skin which comprise the scalp. Interestingly, samples 549 and 559 both showed tubulins as the most abundant proteins rather than keratins. Proteins related to protein folding were highly enriched in 12 of the 21 ancient samples. Peptides belonging to brain and neural-related proteins were found on almost all ancient samples, most likely as a result of the bone and skull fragments being delocalised and heavily disturbed in the coffin as shown in Figure 7 on the following page. It is easy to imagine remaining cellular

material being transferred between bone fragments due to long-term contact over a sustained time period.

Proteins such as vimentin, pyruvate kinase, and transketolase were detected in 10, 13, and 8 of the 21 ancient samples, respectively. These proteins, when expressed in high abundance, have been reported as cancer biomarkers in previous studies [6, 100, 101]. Our ability to detect them approximately 2500 years after the death of the individual, and also given the preservation state of the remains, is suggestive of an increased abundance when the individual was alive. This allows us to speculate regarding cancer as a possible cause of death, which also provides an avenue of investigation for subsequent molecular analysis studies.

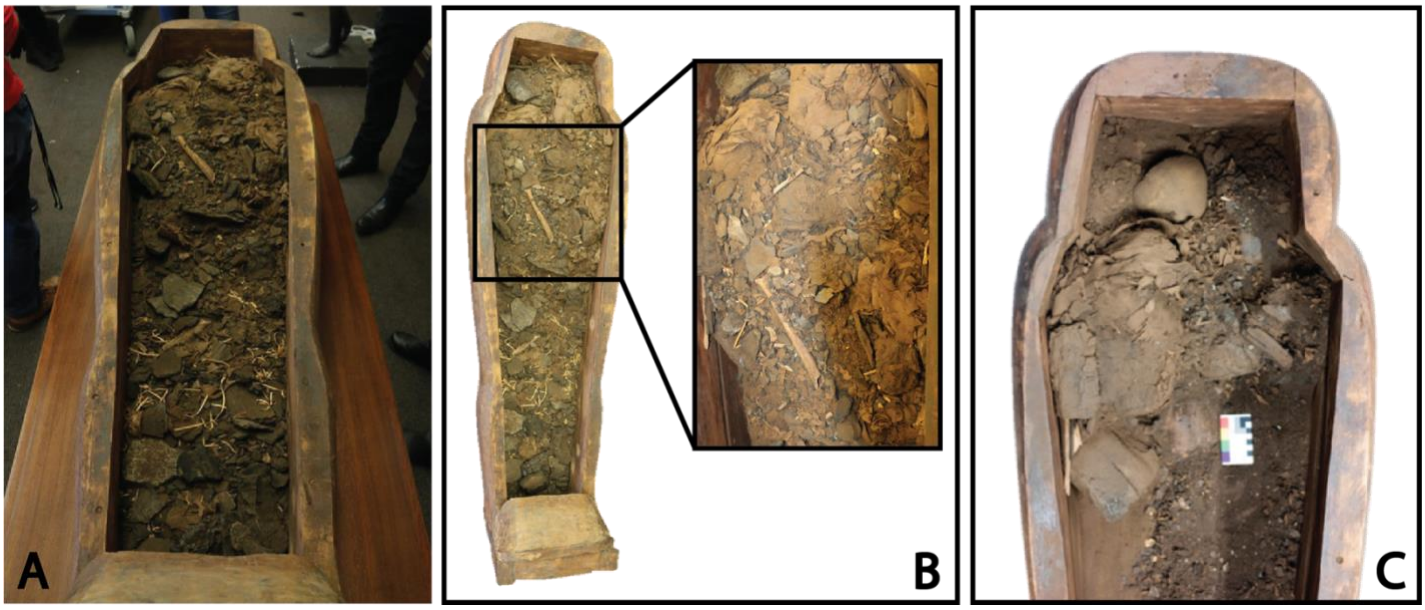

Figure 7 – Images of the contents of NMR.29 coffin, Courtesy of Nicholson Museum. (A) Coffin contents pre-excavation showing extent of disarticulation and fragmentation of skeletal remains and other debris; (B) Coffin contents with close-up of mid-coffin region showing presence of humeral shaft among other bone pieces and debris; (C) Photograph of head-end of coffin mid-excavation showing presence of a skull fragment closely associated with the wrapped feet and tibia. Scale in (C) is 8cm.

4 Conclusion and Future Directions

4.1 Successful proof of concept

First and foremost, it is important to emphasise that the work in this thesis represents a successful proof-of-concept study. When this project began, we had no way of knowing whether the skin sampling strips would be compatible with subsequent protein identification using proteomics analysis techniques. We have demonstrated the feasibility of using dermatology grade skin sampling strips for the proteomic analysis of bioarchaeological materials, by first testing it on modern skin and then applying it to ancient bone samples. Hence, we have developed a novel minimally invasive sampling technique compatible for the proteomic analysis of bioarchaeological materials. Using the methods developed in this thesis, we were able to identify proteins other than the 'usual suspects' of keratins and collagens, including intracellular and brain proteins, which had been extracted from the surface of both modern and ancient samples. The success of this proof-of-concept study holds great promise for subsequent optimisation and application.

4.2 Ideas for further improving the sampling method

We have included in the thesis results of a background control experiment where strips were opened and then extracted in PBS buffer immediately. We also performed more extensive background controls where strips were opened and left with the adhesive side exposed to the laboratory environment for 12-18 hours prior to protein extraction. The results of these experiments were very inconsistent, with some showing high levels of numerous intracellular proteins, while others contained very few proteins. This suggests that airborne protein contaminants may be an issue in the laboratory environment. Thus for future work, it would be ideal to work in a dedicated clean-air laboratory, or at the very least in a dedicated laminar flow hood.

The results presented in this thesis represent approximately 600 hours of dedicated mass spectrometric analysis on a Thermo Q-Exactive mass spectrometer. While the high resolution of this instrument allowed us to detect peptides in the ancient samples, they have been surpassed in resolution and performance by newer machines such as the Thermo Orbitrap Lumos and Eclipse Tribrid Mass Spectrometer. It would be an interesting future project to take ancient protein samples to another mass spectrometric facility and analyse them on these higher-performing instruments to see if the enhanced resolution and sensitivity might yield additional biological information.

The next stage in this project will be to optimise the protein extraction process to maximise efficiency and protein yield. The method used in this thesis was developed based on literature analysis, and due to its success in the sampling and extraction of modern samples, and also the time constraints of this project, it was the only method we investigated. It would be very interesting to perform some more sampling experiments of modern skin and investigate a range of different extraction buffer conditions to see if more proteins could be extracted and identified. Future work could involve testing extraction in various buffers, pH conditions, temperatures and other variables. Another step in the protocol that needs to be optimised is the apparent issue of strip crowding in tubes. This will involve a systematic investigation adjusting extraction solution volume, size of tube used and number of strips per tube in order to maximise protein extraction efficiency and yield from strips. Similarly, the use of SDS-PAGE as a protein fractionation and cleanup technique is based on previous studies from our laboratory [4]. It would also be interesting to investigate alternative sample preparation techniques to see if the results could be improved. For example, extracted proteins could be digested in solution and then fractionated using high pH reversed-phase chromatography prior to nano LC-MS/MS identification of peptides. This could potentially be combined with the recently described workflow based on multiple spin-filtering, which greatly reduces the amount of humic substances in ancient remains and improves protein extraction efficiency [68].

4.3 Ideas for further developing the data analysis method

One recently developed technique we plan to explore is the analysis of glutamine and asparagine deamidation ratios as a complementary relative dating technique [40]. This will involve revisiting the raw MS/MS files using MaxQuant to produce output files compatible with the DeamiDATE software package. Recent preliminary analysis of one dataset from our samples with this software has revealed that there appears to be some variability in the degree of deamidation between proteins, which is possibly an indication of the age of the sample. This software has the potential to help solve one of the real problems in analysing archaeological proteomic data, which is distinguishing ubiquitous modern keratin contaminants from ancient keratins present in sample materials. if we can develop an approach for distinguishing between modern and ancient keratins, it would be a significant advance in the field as it would allow for more accurate filtering of modern contaminants from proteomic data while minimising loss of real ancient protein identifications.

4.4 Ancient remains and non-invasive sampling

This project is part of an ongoing collaboration with Drs Jamie Fraser and Conni Lord from the Nicholson Museum at the University of Sydney, Australia as a part of their interdisciplinary research endeavour, the 'Nicholson Mummy Project'. Due to the fact that we have been able to demonstrate that the non-invasive sampling conducted for this thesis did not cause any obvious damage to the ancient remains, we have permission to sample the Mer-Neith-it-es skull and other bone fragments for further analyses.

One of the main aims of this thesis was to develop a non-invasive sampling method that could then be applied to museum collections across the world to make a wider range of materials available for analysis without destroying them, satisfying the needs of both scientists and curators in archaeology. Once we have developed a fully optimised method and publish the results, we can envisage myriad opportunities for applying this protocol to the analysis of proteins from ancient artefacts in museum collections, including, but not limited to, pottery, animal remains, and preserved soft tissues such as skin. Ancient skin presents a challenge because it is extremely dry and brittle, which is why we chose to start with sampling the surface of bones in this thesis. We have already made contact with several museums regarding the possibility of applying our non-invasive sampling method to remains in their collection, and have had promising discussions concerning a large collection of bone and teeth remains from an enigmatic prehistoric Maltese culture via active research projects within the Department of Ancient History in Macquarie University, and a collection of mummified Sudanese remains housed in the British Museum.

4.5 Finding out more about the enigmatic Mer-Neith-it-es

The sex of the remains of Mer-Neith-it-es is an area of active research and debate within the Nicholson Mummy Project. Currently, this investigation is being performed through the osteological analysis of fragmented bones excavated from the coffin, and the literary analysis of hieroglyphs that adorn the exterior of the burial coffin. These analyses have resulted in conflicting conclusions, and rely on the assumption that the remains belong to the owner of the coffin, which is not necessarily correct. It was apparently quite common in the 19th century for Egyptian traders to sell coffins and mummified bodies, either separately or as a package, to visiting European buyers from museums. Since the coffins containing mummies fetched a higher price, unscrupulous traders were known to put together apparently unrelated artefacts and pass them off as intact units [118].

Within the Mer-Neith-it-es remains there are a number of teeth which could be processed for proteomic analysis. Teeth are a rich resource of biological material when they are sampled destructively, because the dental pulp contained within is often quite well preserved. Recent advances in the use of amelogenin peptide analysis for sex estimation has introduced a new molecular investigative approach to this research question [42]. We would like to explore the future possibility of using a tooth from this collection for proteomic analysis, or possibly DNA-based analysis, to conclusively determine the sex of the remains.

In addition to the skull and other bone strip samples that were collected for this thesis, we were also able to sample several pieces of linen wrapping bandages and crystallised mummification resin of unknown chemical or biological origin collected from the coffin of Mer-Neith-it-es. Initial microscopic analysis of the linen pieces suggests they may be made of flax fibre. We plan to use high resolution mass spectrometry to identify peptides which can provide molecular-level identification of the plant fibre species to complement the initial analyses. The distinction between the use of flax and cotton fibres is important, because only the highest levels of society were mummified in cotton bandages [119, 120]. Furthermore, we hope to use analytical chemistry techniques such as gas chromatography mass spectrometry (GC-MS) and thermal desorption/pyrolysis gas chromatography mass spectrometry (TD/Py-GC-MS) to identify and characterise the chemical nature of the unknown mummification resin [121]. The composition of the resin used can provide important information about the societal status of the individual, based on the materials used and their geographic origins [122, 123].

4.6 Conclusions

In this thesis, we have successfully developed a non-destructive sampling technique for proteomics analysis of ancient bone samples, which is based on applying dermatological skin sampling strips to the surface of bones. We have shown that we can successfully identify intracellular proteins from skull fragments and other bones from the mummified ancient Egyptian remains Mer-Neith-it-es. There is still plenty of room for further optimisation and improvement of the methods involved, but it represents a very promising start. Our goal is to continue developing and optimising new molecular analysis methods which can be used to generate information which furthers our understanding of life and death in ancient cultures. This synthesis of biochemical analysis with archaeological study represents the archetype of the emerging discipline of bioarchaeological proteomics.

References

[1] Brown, K. A., Brown, T. A., Biomolecular Archaeology. *Annual Review of Anthropology* 2013, *42*, 159-174.
[2] van Schaik, K., Eisenberg, R., Bekvalac, J., Rühli, F., The Radiologist in the Crypt: Burden of Disease in the Past and Its Modern Relevance. *Academic Radiology* 2017, *24*, 1305-1311.
[3] Corthals, A., Koller, A., Martin, D. W., Rieger, R., Chen, E. I., Bernaski, M., Recagno, G., Dávalos, L. M., Detecting the Immune System Response of a 500 Year-Old Inca Mummy (Pathogen Detection Using Proteomics). *PLoS ONE* 2012, *7*, e41244.
[4] Jones, J., Mirzaei, M., Ravishankar, P., Xavier, D., Lim do, S., Shin, D. H., Bianucci, R., Haynes, P. A., Identification of proteins from 4200-year-old skin and muscle tissue biopsies from ancient Egyptian mummies of the first intermediate period shows evidence of acute inflammation and severe immune response. *Philosophical Transactions of the Royal Society A* 2016, *374*.
[5] Solazzo, C., Fitzhugh, W. W., Rolando, C., Tokarski, C., Identification of Protein Remains in Archaeological Potsherds by Proteomics. *Analytical Chemistry* 2008, *80*, 4590-4597.
[6] Bona, A., Papai, Z., Maasz, G., Toth, G. A., Jambor, E., Schmidt, J., Toth, C., Farkas, C., Mark, L., Mass Spectrometric Identification of Ancient Proteins as Potential Molecular Biomarkers for a 2000-Year-Old Osteogenic Sarcoma. *PLoS ONE* 2014, *9*.
[7] Hendy, J., Warinner, C., Bouwman, A., Collins, M. J., Fiddyment, S., Fischer, R., Hagan, R., Hofman, C. A., Holst, M., Chaves, E., Klaus, L., Larson, G., Mackie, M., McGrath, K., Mundorff, A. Z., Radini, A., Rao, H., Trachsel, C., Velsko, I. M., Speller, C. F., Proteomic evidence of dietary sources in ancient dental calculus. *Proceedings of the Royal Society B: Biological Sciences* 2018, *285*.
[8] Li, L., Gong, Y., Yin, H., Gong, D., Different Types of Peptide Detected by Mass Spectrometry among Fresh Silk and Archaeological Silk Remains for Distinguishing Modern Contamination. *PLoS ONE* 2015, *10*.
[9] Dewitte, S. N., Bioarchaeology and the Ethics of Research Using Human Skeletal Remains. *History Compass* 2015, *13*, 10-19.
[10] Kaestle, F. A., Horsburgh, K. A., Ancient DNA in anthropology: Methods, applications, and ethics. *American Journal of Physical Anthropology* 2002, *119*, 92-130.
[11] Weyrich, L. S., Duchene, S., Soubrier, J., Arriola, L., Llamas, B., Breen, J., Morris, A. G., Alt, K. W., Caramelli, D., Dresely, V., Farrell, M., Farrer, A. G., Francken, M., Gully, N., Haak, W., Hardy, K., Harvati, K., Held, P., Holmes, E. C., Kaidonis, J., Lalueza-Fox, C., de la Rasilla, M., Rosas, A., Semal, P., Soltysiak, A., Townsend, G., Usai, D., Wahl, J., Huson, D. H., Dobney, K., Cooper, A., Neanderthal behaviour, diet, and disease inferred from ancient DNA in dental calculus. *Nature* 2017, *544*, 357.
[12] Boros-Major, A., Bona, A., Lovasz, G., Molnar, E., Marcsik, A., Palfi, G., Mark, L., New perspectives in biomolecular paleopathology of ancient tuberculosis: a proteomic approach. *Journal of Archaeological Science* 2011, *38*, 197-201.
[13] DeWitte, S. N., Archaeological Evidence of Epidemics Can Inform Future Epidemics. *Annual Review of Anthropology* 2016, *45*, 63-77.
[14] Walker, P. L., in: Katzenberg, M., Saunders, S. (Ed.), *Biological Anthropology of the Human Skeleton*, Wiley-Liss, Wilmington 2008, pp. 3-39.
[15] Appenzeller, O., Bromage, T. G., Khairat, R., Nerlich, A. G., Rühli, F. J., Bioarcheology: Medicine, Biology, and Forensic Sciences. *BioMed Research International* 2015, *2015*.

[16] Larsen, C., Bioarchaeology: The Lives and Lifestyles of Past People. *Journal of Archaeological Research* 2002, *10*, 119-166.
[17] Somerville, A. D., Goldstein, P. S., Baitzel, S. I., Bruwelheide, K. L., Dahlstedt, A. C., Yzurdiaga, L., Raubenheimer, S., Knudson, K. J., Schoeninger, M. J., Diet and gender in the Tiwanaku colonies: Stable isotope analysis of human bone collagen and apatite from Moquegua, Peru. *American Journal of Physical Anthropology* 2015, *158*, 408-422.
[18] Rácz, S. E., Pucu De Araújo, E., Jensen, E., Mostek, C., Morrow, J. J., Van Hove, M. L., Bianucci, R., Willems, D., Heller, F., Araújo, A., Reinhard, K. J., Parasitology in an archaeological context: analysis of medieval burials in Nivelles, Belgium. *Journal of Archaeological Science* 2015, *53*, 304 - 315.
[19] Rizzi, E., Lari, M., Gigli, E., De Bellis, G., Caramelli, D. J. G. S. E., Ancient DNA studies: new perspectives on old samples. *Genetics, Selection, Evolution* 2012, *44*, 21.
[20] Higuchi, R., Bowman, B., Freiberger, M., Ryder, O. A., Wilson, A. C., DNA sequences from the quagga, an extinct member of the horse family. *Nature* 1984, *312*, 282.
[21] Green, R. E., Krause, J., Briggs, A. W., Maricic, T., Stenzel, U., Kircher, M., Patterson, N., Li, H., Zhai, W., Fritz, M. H.-Y., Hansen, N. F., Durand, E. Y., Malaspinas, A.-S., Jensen, J. D., Marques-Bonet, T., Alkan, C., Prüfer, K., Meyer, M., Burbano, H. A., Good, J. M., Schultz, R., Aximu-Petri, A., Butthof, A., Höber, B., Höffner, B., Siegemund, M., Weihmann, A., Nusbaum, C., Lander, E. S., Russ, C., Novod, N., Affourtit, J., Egholm, M., Verna, C., Rudan, P., Brajkovic, D., Kucan, Ž., Gušic, I., Doronichev, V. B., Golovanova, L. V., Lalueza-Fox, C., de la Rasilla, M., Fortea, J., Rosas, A., Schmitz, R. W., Johnson, P. L. F., Eichler, E. E., Falush, D., Birney, E., Mullikin, J. C., Slatkin, M., Nielsen, R., Kelso, J., Lachmann, M., Reich, D., Pääbo, S., A Draft Sequence of the Neandertal Genome. *Science* 2010, *328*, 710.
[22] Warinner, C., Speller, C., Collins, M. J., Lewis, C. M., Ancient human microbiomes. *Journal of Human Evolution* 2015, *79*, 125-136.
[23] Drancourt, M., Raoult, D., Molecular insights into the history of plague. *Microbes and Infection* 2002, *4*, 105-109.
[24] Harbeck, M., Seifert, L., Hänsch, S., Wagner, D. M., Birdsell, D., Parise, K. L., Wiechmann, I., Grupe, G., Thomas, A., Keim, P., Zöller, L., Bramanti, B., Riehm, J. M., Scholz, H. C., Yersinia pestis DNA from skeletal remains from the 6th century AD reveals insights into Justinianic Plague. *PLoS pathogens* 2013, *9*, e1003349-e1003349.
[25] Deguilloux, M.-F., Pemonge, M.-H., Dubut, V., Hughes, S., Hänni, C., Chollet, L., Conte, E., Murail, P., Human ancient and extant mtDNA from the Gambier Islands (French polynesia): Evidence for an early Melanesian maternal contribution and new perspectives into the settlement of Easternmost Polynesia. *American Journal of Physical Anthropology* 2011, *144*, 248-257.
[26] Matisoo-Smith, E., Ancient DNA and the human settlement of the Pacific: A review. *Journal of Human Evolution* 2015, *79*, 93-104.
[27] Hofreiter, M., Serre, D., Poinar, H. N., Kuch, M., Pääbo, S., Ancient DNA. *Nature reviews. Genetics* 2001, *2*, 353.
[28] Lindahl, T., Instability and decay of the primary structure of DNA. *Nature* 1993, *362*, 709.
[29] Dallongeville, S., Garnier, N., Rolando, C., Tokarski, C., Proteins in Art, Archaeology, and Paleontology: From Detection to Identification. *Chemical Reviews* 2016, *116*, 2-79.
[30] Service, R. F., Protein power. *Science* 2015, *349*, 372.
[31] Wallace, A. F., Schiffbauer, J. D., Proteins from the past. *eLife* 2016, *5*, e20877.
[32] Wiecek, A. S., Rewriting history through proteins. *Biotechniques* 2013, *54*, 19-21.
[33] Andrew, S. W., Emma, L. B., Chiara, V., Niels, L., Andrew, H., Maria Constanza, C., Johan, R., Carlos, H. P., Facundo Arias, A., Josefina Gonzalez, D., Timothy, T.,

Archaeological, radiological, and biological evidence offer insight into Inca child sacrifice. *Proceedings of the National Academy of Sciences* 2013, *110*, 13322.
[34] Harvey, V., Egerton, V., Chamberlain, A., Manning, P., Buckley, M., Collagen Fingerprinting: A New Screening Technique for Radiocarbon Dating Ancient Bone: e0150650. *PLoS ONE* 2016, *11*.
[35] Buckley, M., Collins, M., Thomas-Oates, J., Wilson, J. C., Species identification by analysis of bone collagen using matrix-assisted laser desorption/ionisation time-of-flight mass spectrometry. *Rapid Communications in Mass Spectrometry* 2009, *23*, 3843-3854.
[36] Buckley, M., Fraser, S., Herman, J., Melton, N. D., Mulville, J., Pálsdóttir, A. H., Species identification of archaeological marine mammals using collagen fingerprinting. *Journal of Archaeological Science* 2014, *41*, 631-641.
[37] Wadsworth, C., Buckley, M., Proteome degradation in fossils: investigating the longevity of protein survival in ancient bone. *Rapid Communications in Mass Spectrometry* 2014, *28*, 605-615.
[38] Buckley, M., Whitcher Kansa, S., Howard, S., Campbell, S., Thomas-Oates, J., Collins, M., Distinguishing between archaeological sheep and goat bones using a single collagen peptide. *Journal of Archaeological Science* 2010, *37*, 13-20.
[39] Buckley, M., Larkin, N., Collins, M., Mammoth and Mastodon collagen sequences; survival and utility. *Geochimica et Cosmochimica Acta* 2011, *75*, 2007-2016.
[40] Ramsøe, A., DeamiDATE 1.0: Site-specific deamidation as a tool to assess authenticity of members of ancient proteomes. *Proceedings of 67th ASMS Conference on Mass Spectrometry & Allied Topics* 2019.
[41] Pal Chowdhury, M., Wogelius, R., Manning, P. L., Metz, L., Slimak, L., Buckley, M., Collagen deamidation in archaeological bone as an assessment for relative decay rates. *Archaeometry* 2019, 1382-1398.
[42] Parker, G. J., Yip, J. M., Eerkens, J. W., Salemi, M., Durbin-Johnson, B., Kiesow, C., Haas, R., Buikstra, J. E., Klaus, H., Regan, L. A., Rocke, D. M., Phinney, B. S., Sex estimation using sexually dimorphic amelogenin protein fragments in human enamel. *Journal of Archaeological Science* 2019, *101*, 169-180.
[43] Mazumder, P., Prajapati, S., Lokappa, S. B., Gallon, V., Moradian-Oldak, J., Analysis of co-assembly and co-localization of ameloblastin and amelogenin. *Frontiers in Physiology* 2014, *5*.
[44] Schweitzer Mary, H., Zheng, W., Cleland Timothy, P., Goodwin Mark, B., Boatman, E., Theil, E., Marcus Matthew, A., Fakra Sirine, C., A role for iron and oxygen chemistry in preserving soft tissues, cells and molecules from deep time. *Proceedings of the Royal Society B: Biological Sciences* 2014, *281*, 20132741.
[45] Schweitzer, M. H., Zheng, W., Moyer, A. E., Sjövall, P., Lindgren, J., Preservation potential of keratin in deep time. *PLoS ONE* 2018, *13*, e0206569-e0206569.
[46] Avci, R., Schweitzer, M. H., Boyd, R. D., Wittmeyer, J. L., Terán Arce, F., Calvo, J. O., Preservation of Bone Collagen from the Late Cretaceous Period Studied by Immunological Techniques and Atomic Force Microscopy. *Langmuir* 2005, *21*, 3584-3590.
[47] Bertazzo, S., Maidment, S. C. R., Kallepitis, C., Fearn, S., Stevens, M. M., Xie, H.-n., Fibres and cellular structures preserved in 75-million-year-old dinosaur specimens. *Nature Communications* 2015, *6*, 7352-7352.
[48] Crane, P. R., Friis, E. M., Fossils and Plant Phylogeny. *American Journal of Botany* 2004, *91*, 1683-1699.
[49] Schweitzer, M. H., Wittmeyer, J. L., Horner, J. R., Toporski, J. K., Soft-Tissue Vessels and Cellular Preservation in Tyrannosaurus rex. *Science* 2005, *307*, 1952-1955.

[50] Schweitzer, M. H., Suo, Z., Avci, R., Asara, J. M., Allen, M. A., Arce, F. T., Horner, J. R., Analyses of Soft Tissue from *Tyrannosaurus rex* Suggest the Presence of Protein. *Science* 2007, *316*, 277.
[51] San Antonio, J. D., Schweitzer, M. H., Jensen, S. T., Kalluri, R., Buckley, M., Orgel, J. P. R. O., Dinosaur peptides suggest mechanisms of protein survival. *PLoS ONE* 2011, *6*, 20381-20387.
[52] Schweitzer, M. H., Moyer, A. E., Zheng, W., Testing the Hypothesis of Biofilm as a Source for Soft Tissue and Cell-Like Structures Preserved in Dinosaur Bone. *PLoS ONE* 2016, *11*, e0150238-e0150238.
[53] Schweitzer, M. H., Schroeter, E. R., Goshe, M. B., Protein Molecular Data from Ancient (>1 million years old) Fossil Material: Pitfalls, Possibilities and Grand Challenges. *Analytical Chemistry* 2014, *86*, 6731-6740.
[54] Asara, J. M., Schweitzer, M. H., Freimark, L. M., Phillips, M., Cantley, L. C., Protein Sequences from Mastodon and Tyrannosaurus Rex Revealed by Mass Spectrometry. *Science* 2007, *316*, 280-285.
[55] Gee, B. M., Bevitt, J. J., Garbe, U., Reisz, R. R., New material of the 'microsaur' Llistrofus from the cave deposits of Richards Spur, Oklahoma and the paleoecology of the Hapsidopareiidae. *PeerJ* 2019, *7*, e6327-e6327.
[56] Schreiner, M., Frühmann, B., Jembrih-Simbürger, D., Linke, R., X-rays in art and archaeology: An overview. *Powder Diffraction* 2004, *19*, 3-11.
[57] Sanger, M. C., Investigating pottery vessel manufacturing techniques using radiographic imaging and computed tomography: Studies from the Late Archaic American Southeast. *Journal of Archaeological Science: Reports* 2016, *9*, 586-598.
[58] Barberis, E., Baiocco, S., Conte, E., Gosetti, F., Rava, A., Zilberstein, G., Righetti, P. G., Marengo, E., Manfredi, M., Towards the non-invasive proteomic analysis of cultural heritage objects. *Microchemical Journal* 2018, *139*, 450-457.
[59] Manfredi, M., Barberis, E., Gosetti, F., Conte, E., Gatti, G., Mattu, C., Robotti, E., Zilberstein, G., Koman, I., Zilberstein, S., Marengo, E., Righetti, P. G., Method for Noninvasive Analysis of Proteins and Small Molecules from Ancient Objects. *Analytical Chemistry* 2017, *89*, 3310-3317.
[60] Moodley, A., Espinosa-Gongora, C., Nielsen, S. S., McCarthy, A. J., Lindsay, J. A., Guardabassi, L., Comparative Host Specificity of Human- and Pig- Associated Staphylococcus aureus Clonal Lineages (Host Specificity of S. aureus). *PLoS ONE* 2012, *7*, e49344.
[61] Stroh, A., Werckenthin, C., Luis, C. S., Mueller, R. S., Influence of a phytosphingosine-containing chlorhexidine shampoo on superficial bacterial counts and bacterial adherence to canine keratinocytes. *Veterinary Microbiology* 2010, *141*, 190-193.
[62] Berdyshev, E., Goleva, E., Bronova, I., Dyjack, N., Rios, C., Jung, J., Taylor, P., Jeong, M., Hall, C., Richers, B., Norquest, K., Zheng, T., Seibold, M. A., Leung, D., Lipid abnormalities in atopic skin are driven by type 2 cytokines. *JCI Insight* 2018, *3*.
[63] Broccardo, C. J., Mahaffey, S. B., Strand, M., Reisdorph, N. A., Leung, D. Y. M., Peeling off the layers: Skin taping and a novel proteomics approach to study atopic dermatitis. *Journal of Allergy and Clinical Immunology* 2009, *124*, 1113-1115.e1111.
[64] Rana, G. E.-R., Helen, S. Y., Christopher, E. M. G., Richard, D. R. C., Humoral Autoimmune Responses to the Squamous Cell Carcinoma Antigen Protein Family in Psoriasis. *Journal of Investigative Dermatology* 2008, *128*, 2219.
[65] Karim, N., Durbin-Johnson, B., Rocke, D. M., Salemi, M., Phinney, B. S., Naeem, M., Rice, R. H., Proteomic manifestations of genetic defects in autosomal recessive congenital ichthyosis. *Journal of Proteomics* 2019, *201*, 104-109.

[66] Trendall, A. D., *Handbook to the Nicholson Museum*, University of Sydney, Sydney 1945.
[67] Clausen, M.-L., Slotved, H. C., Krogfelt, K. A., Agner, T., Tape Stripping Technique for Stratum Corneum Protein Analysis. *Scientific Reports* 2016, *6*, 19918-19918.
[68] Schroeter, E. R., Blackburn, K., Goshe, M. B., Schweitzer, M. H., A Proteomic Workflow to Extract, Concentrate, Digest, and Enrich Peptides from Fossils with High Humic Content for Mass Spectrometry Analyses. *Proceedings of 67th ASMS Conference on Mass Spectrometry & Allied Topics.* 2019.
[69] Koster, J., Geerts, D., Favre, B., Borradori, L., Sonnenberg, A., Analysis of the interactions between BP180, BP230, plectin and the integrin alpha6beta4 important for hemidesmosome assembly. *Journal of Cell Science* 2003, *116*, 387-399.
[70] Fujita, M., Mitsuhashi, H., Isogai, S., Nakata, T., Kawakami, A., Nonaka, I., Noguchi, S., Hayashi, Y. K., Nishino, I., Kudo, A., Filamin C plays an essential role in the maintenance of the structural integrity of cardiac and skeletal muscles, revealed by the medaka mutant zacro. *Developmental Biology* 2012, *361*, 79-89.
[71] Chen, Y., Gaczynska, M., Osmulski, P., Polci, R., Riley, D. J., Phosphorylation by Nek1 regulates opening and closing of voltage dependent anion channel 1. *Biochemical and Biophysical Research Communications* 2010, *394*, 798-803.
[72] Tamás, B.-S., Per, L., Bengt, N., Rate of hydrolysis in ATP synthase is fine-tuned by α-subunit motif controlling active site conformation. *Proceedings of the National Academy of Sciences* 2013, *110*, 2117.
[73] Coates, P. J., Nenutil, R., McGregor, A., Picksley, S. M., Crouch, D. H., Hall, P. A., Wright, E. G., Mammalian prohibitin proteins respond to mitochondrial stress and decrease during cellular senescence. *Experimental Cell Research* 2001, *265*, 262-273.
[74] Sensenbrenner, M., Lucas, M., Deloulme, J.-C. J. J. o. M. M., Expression of two neuronal markers, growth-associated protein 43 and neuron-specific enolase, in rat glial cells. *Journal of Molecular Medicine* 1997, *75*, 653-663.
[75] Drikes, S., Delcampe, P., Sabin, P., Lavis, J. F., Cordier, G., Vacher, C., Péron, J. M., CT scan study of the mandibular nerve intra-mandibular path. *Revue de Stomatologie et de Chirurgie Maxillo-faciale* 2011, *112*, e5-e10.
[76] Yu, D. F., Chen, Y., Han, J. M., Zhang, H., Chen, X. P., Zou, W. J., Liang, L. Y., Xu, C. C., Liu, Z. G., MUC19 expression in human ocular surface and lacrimal gland and its alteration in Sjogren syndrome patients. *Experimental Eye Research* 2008, *86*, 403-411.
[77] Berns, D. S., DeNardo, L. A., Pederick, D. T., Luo, L., Teneurin-3 controls topographic circuit assembly in the hippocampus. *Nature* 2018, *554*, 328.
[78] Chen, X.-Q., Fang, F., Florio, J. B., Rockenstein, E., Masliah, E., Mobley, W. C., Rissman, R. A., Wu, C., T-complex protein 1-ring complex enhances retrograde axonal transport by modulating tau phosphorylation. *Traffic* 2018, *19*, 840-853.
[79] Freund, A., Zhong, F. L., Venteicher, A. S., Meng, Z., Veenstra, T. D., Frydman, J., Artandi, S. E., Proteostatic control of telomerase function through TRiC-mediated folding of TCAB1. *Cell* 2014, *159*, 1389-1403.
[80] Hirokawa, N., Sobue, K., Kanda, K., Harada, A., Yorifuji, H., The cytoskeletal architecture of the presynaptic terminal and molecular structure of synapsin 1. *The Journal of Cell Biology* 1989, *108*, 111-126.
[81] Asperti, C., Astro, V., Pettinato, E., Paris, S., Bachi, A., de Curtis, I., Biochemical and Functional Characterization of the Interaction between Liprin-[alpha]1 and GIT1: Implications for the Regulation of Cell Motility.(Research Article). *PLoS ONE* 2011, *6*, e20757.

[82] Pasupala, N., Morrow, M. E., Que, L. T., Malynn, B. A., Ma, A., Wolberger, C., OTUB1 non-catalytically stabilizes the E2 ubiquitin-conjugating enzyme UBE2E1 by preventing its autoubiquitination. *The Journal of Biological Chemistry* 2018, *293*, 18285.
[83] Ikegawa, S., Sudo, K., Okui, K., Nakamura, Y., Isolation, characterization and chromosomal assignment of human colligin-2 gene (CBP2). *Cytogenetics and Cell Genetics* 1995, *71*, 182-186.
[84] Davis, T. L., Walker, J. R., Campagna-Slater, V., Finerty, P. J., Paramanathan, R., Bernstein, G., MacKenzie, F., Tempel, W., Ouyang, H., Lee, W. H., Eisenmesser, E. Z., Dhe-Paganon, S., Structural and biochemical characterization of the human cyclophilin family of peptidyl-prolyl isomerases. *PLoS Biology* 2010, *8*, e1000439.
[85] Maggi, L. B., Jr., Kuchenruether, M., Dadey, D. Y., Schwope, R. M., Grisendi, S., Townsend, R. R., Pandolfi, P. P., Weber, J. D., Nucleophosmin serves as a rate-limiting nuclear export chaperone for the Mammalian ribosome. *Molecular and Cellular Biology* 2008, *28*, 7050-7065.
[86] Bai, S. W., Herrera-Abreu, M. T., Rohn, J. L., Racine, V., Tajadura, V., Suryavanshi, N., Bechtel, S., Wiemann, S., Baum, B., Ridley, A. J., Identification and characterization of a set of conserved and new regulators of cytoskeletal organization, cell morphology and migration. *BMC Biology* 2011, *9*, 54.
[87] Sun, K. H., Chang, K. H., Clawson, S., Ghosh, S., Mirzaei, H., Regnier, F., Shah, K., Glutathione-S-transferase P1 is a critical regulator of Cdk5 kinase activity. *Journal of Neurochemistry* 2011, *118*, 902-914.
[88] Pieragostino, D., Agnifili, L., Fasanella, V., D'Aguanno, S., Mastropasqua, R., Di Ilio, C., Sacchetta, P., Urbani, A., Del Boccio, P., Shotgun proteomics reveals specific modulated protein patterns in tears of patients with primary open angle glaucoma naive to therapy. *Molecular Biosystems* 2013, *9*, 1108-1116.
[89] Ericksen, B., Wu, Z., Lu, W., Lehrer, R. I., Antibacterial activity and specificity of the six human {alpha}-defensins. *Antimicrobial Agents and Chemotherapy* 2005, *49*, 269-275.
[90] Tollin, M., Bergman, P., Svenberg, T., Jornvall, H., Gudmundsson, G. H., Agerberth, B., Antimicrobial peptides in the first line defence of human colon mucosa. *Peptides* 2003, *24*, 523-530.
[91] Henry, J., Hsu, C. Y., Haftek, M., Nachat, R., de Koning, H. D., Gardinal-Galera, I., Hitomi, K., Balica, S., Jean-Decoster, C., Schmitt, A. M., Paul, C., Serre, G., Simon, M., Hornerin is a component of the epidermal cornified cell envelopes. *FASEB Journal* 2011, *25*, 1567-1576.
[92] Dana, R. C., Welch, W. J., Deftos, L. J., Heat shock proteins bind calcitonin. *Endocrinology* 1990, *126*, 672-674.
[93] Parada, C. A., Roeder, R. G., A novel RNA polymerase II-containing complex potentiates Tat-enhanced HIV-1 transcription. *EMBO Journal* 1999, *18*, 3688-3701.
[94] Chan, S. O., Chiu, F. C., Cloning and developmental expression of human 66 kd neurofilament protein. *Molecular Brain Research* 1995, *29*, 177-184.
[95] Hyunook, K., Thomas, M. W., Injin, B., William, I. W., Hee-Jung, C., Structure of the Intermediate Filament-Binding Region of Desmoplakin. *PLoS ONE* 2016, *11*, e0147641.
[96] Mayer, G., Poirier, S., Seidah, N. G., Annexin A2 is a C-terminal PCSK9-binding protein that regulates endogenous low density lipoprotein receptor levels. *Journal of Biological Chemistry* 2008, *283*, 31791-31801.
[97] Ying, X., Peng, Y., Zhang, J., Wang, X., Wu, N., Zeng, Y., Wang, Y., Endogenous α-crystallin inhibits expression of caspase-3 induced by hypoxia in retinal neurons. *Life Sciences* 2014, *111*, 42-46.

[98] Nye, S. H., Pelfrey, C. M., Burkwit, J. J., Voskuhl, R. R., Lenardo, M. J., Mueller, J. P., Purification of immunologically active recombinant 21.5 kDa isoform of human myelin basic protein. *Molecular Immunology* 1995, *32*, 1131-1141.
[99] Challa, A. A., Stefanovic, B., A novel role of vimentin filaments: binding and stabilization of collagen mRNAs. *Molecular and Cellular Biology* 2011, *31*, 3773-3789.
[100] Boyle, L., Wamelink, M. M. C., Salomons, G. S., Roos, B., Pop, A., Dauber, A., Hwa, V., Andrew, M., Douglas, J., Feingold, M., Kramer, N., Saitta, S., Retterer, K., Cho, M. T., Begtrup, A., Monaghan, K. G., Wynn, J., Chung, W. K., Mutations in TKT Are the Cause of a Syndrome Including Short Stature, Developmental Delay, and Congenital Heart Defects. *American Journal of Human Genetics* 2016, *98*, 1235-1242.
[101] Stetak, A., Veress, R., Ovadi, J., Csermely, P., Keri, G., Ullrich, A., Nuclear translocation of the tumor marker pyruvate kinase M2 induces programmed cell death. *Cancer Research* 2007, *67*, 1602-1608.
[102] Royle, S. J., Bright, N. A., Lagnado, L., Clathrin is required for the function of the mitotic spindle. *Nature* 2005, *434*, 1152-1157.
[103] Ravikumar, B., Moreau, K., Jahreiss, L., Puri, C., Rubinsztein, D. C., Plasma membrane contributes to the formation of pre-autophagosomal structures. *Nature Cell Biology* 2010, *12*, 747-757.
[104] Ferguson, S. M., Brasnjo, G., Hayashi, M., Wölfel, M., Collesi, C., Giovedi, S., Raimondi, A., Gong, L.-W., Ariel, P., Paradise, S., Toole, E., Flavell, R., Cremona, O., Miesenböck, G., Ryan, T. A., De Camilli, P., A Selective Activity-Dependent Requirement for Dynamin 1 in Synaptic Vesicle Endocytosis. *Science* 2007, *316*, 570.
[105] Wolf, A. J., Reyes, C. N., Liang, W., Becker, C., Shimada, K., Wheeler, M. L., Cho, H. C., Popescu, N. I., Coggeshall, K. M., Arditi, M., Underhill, D. M., Hexokinase Is an Innate Immune Receptor for the Detection of Bacterial Peptidoglycan. *Cell* 2016, *166*, 624-636.
[106] Matsuura, K., Nakamura-Hirota, T., Takano, M., Otani, M., Kadoyama, K., Matsuyama, S., Proteomic analysis of time-dependent changes in proteins expressed in mouse hippocampus during synaptic plasticity induced by GABAA receptor blockade. *Neuroscience Letters* 2013, *555*, 18-23.
[107] Lim, S.-H., Moon, J., Lee, M., Lee, J.-R., PTPRT regulates the interaction of Syntaxin-binding protein 1 with Syntaxin 1 through dephosphorylation of specific tyrosine residue. *Biochemical and Biophysical Research Communications* 2013, *439*, 40-46.
[108] Hall, P. A., Jung, K., Hillan, K. J., Russell, S. E., Expression profiling the human septin gene family. *Journal of Pathology* 2005, *206*, 269-278.
[109] Reid, R. A., Bronson, D. D., Young, K. M., Hemperly, J. J., Identification and characterization of the human cell adhesion molecule contactin. *Molecular Brain Research* 1994, *21*, 1-8.
[110] Wasenius, V. M., Saraste, M., Salvén, P., Erämaa, M., Holm, L., Lehto, V. P., Primary structure of the brain alpha-spectrin. *The Journal of Cell Biology* 1989, *108*, 79-93.
[111] Myllykoski, M., Seidel, L., Muruganandam, G., Raasakka, A., Torda, A. E., Kursula, P., Structural and functional evolution of 2′,3′-cyclic nucleotide 3′-phosphodiesterase. *Brain Research* 2016, *1641*, 64-78.
[112] Betapudi, V., Myosin II motor proteins with different functions determine the fate of lamellipodia extension during cell spreading. *PLoS ONE* 2010, *5*, e8560.
[113] Huang, T. Y., Minamide, L. S., Bamburg, J. R., Bokoch, G. M., Chronophin Mediates an ATP-Sensing Mechanism for Cofilin Dephosphorylation and Neuronal Cofilin-Actin Rod Formation. *Developmental Cell* 2008, *15*, 691-703.
[114] Benaud, C., Gentil, B. J., Assard, N., Court, M., Garin, J., Delphin, C., Baudier, J., AHNAK interaction with the annexin 2/S100A10 complex regulates cell membrane cytoarchitecture. *Journal of Cell Biology* 2004, *164*, 133-144.

[115] Aitken, A., Collinge, D. B., van Heusden, B. P. H., Isobe, T., Roseboom, P. H., Rosenfeld, G., Soll, J., 14-3-3 proteins: a highly conserved, widespread family of eukaryotic proteins. *Trends in Biochemical Sciences* 1992, *17*, 498-501.
[116] Ercolani, L., Florence, B., Denaro, M., Alexander, M., Isolation and complete sequence of a functional human glyceraldehyde-3-phosphate dehydrogenase gene. *Journal of Biological Chemistry* 1988, *263*, 15335-15341.
[117] Sakoda, S., Shanske, S., DiMauro, S., Schon, E. A., Isolation of a cDNA encoding the B isozyme of human phosphoglycerate mutase (PGAM) and characterization of the PGAM gene family. *Journal of Biological Chemistry* 1988, *263*, 16899-16905.
[118] Fraser, J., *Nicholson Museum Mummy Project Symposium*, University of Sydney, University of Sydney, Sydney, Australia 2019.
[119] Lucas, A., Problems in connection with ancient Egyptian materials. *Analyst* 1926, *51*, 435-450.
[120] Gardner, J. C., Garvin, G., Nelson, A. J., Vascotto, G., Conlogue, G., Paleoradiology in mummy studies: the Sulman mummy project. *Canadian Association of Radiologists journal = Journal l'Association canadienne des radiologistes* 2004, *55*, 228.
[121] Jana, J., Thomas, F. G. H., Ron, O., Terry, P. O. C., Stephen, A. B., Evidence for prehistoric origins of Egyptian mummification in late Neolithic burials. *PLoS ONE* 2014, *9*, e103608.
[122] Buckley, S. A., Evershed, R. P., Organic chemistry of embalming agents in Pharaonic and Graeco-Roman mummies. *Nature* 2001, *413*, 837-841.
[123] Buckley, S. A., Clark, K. A., Evershed, R. P., Complex organic chemical balms of Pharaonic animal mummies. *Nature* 2004, *431*, 294-299.

Appendix 1: CloudStor repository of raw MS/MS files and unfiltered GPM outputs

Raw MS/MS files and unfiltered GPM outputs were uploaded to a CloudStor repository (accessible at: https://cloudstor.aarnet.edu.au/plus/s/rRdouERweRcCI0j).

This repository contains 8 folders each labelled with a 6-digit numerical code and brief description of the sample (e.g. 190516_ancient_skull_1034_1134). Each of these folders contains a folder entitled 'Raw', which contains the .raw MS/MS files from the Q-Exactive mass spectrometer, and a .xlsx spreadsheet of the unfiltered corresponding GPM outputs for those samples.

Each individual sample is represented by 8 .raw files which correspond to the 8 SDS-PAGE gel fractions.

Appendix 2 (page 60) removed from Open Access version as it/they may contain sensitive/confidential content.